The matrix product approach to quantum spin ladders

1998 J. Phys. A: Math. Gen. 31 9729

(http://iopscience.iop.org/0305-4470/31/48/009)

J. Phys. A: Math. Gen. **31** (1998) 9729–9759. Printed in the UK PII: S0305-4470(98)93004-9

The matrix product approach to quantum spin ladders

J M Román†, G Sierra‡, J Dukelsky§ and M A Martín-Delgado‖

† Departament d'ECM, Universitat de Barcelona, Barcelona, Spain
‡ Instituto de Matemáticas y Física Fundamental, CSIC, Madrid, Spain
§ Instituto de Estructura de la Materia, CSIC, Madrid, Spain
‖ Departamento de Física Teórica I, Universidad Complutense, Madrid, Spain

Received 1 April 1998, in final form 1 September 1998

Abstract. We present a manifestly rotational invariant formulation of the matrix product method valid for spin chains and ladders. We apply it to two-legged spin ladders with spins $\frac{1}{2}$, 1 and $\frac{3}{2}$ and different magnetic structures labelled by the exchange coupling constants, which can be ferromagnetic or antiferromagnetic along the legs and the rungs of the ladder. We compute ground-state energy densities, correlation lengths and string order parameters. We present numerical evidence of the duality properties of the three different nonferromagnetic spin $\frac{1}{2}$ ladders. We show that the long-range topological order characteristic of isolated spin 1 chains is broken by the interchain coupling. The string order correlation function decays exponentially with a finite correlation length that we compute. A physical picture of the spin 1 ladder is given in terms of a collection of resonating spin 1 chains. Finally, for ladders with spin equal to or greater than $\frac{3}{2}$ we define a class of AKLT states whose matrix product coefficients are given by 9-j symbols.

1. Introduction

The matrix product method (MPM) is a variational approach appropiate to study the ground state (GS) and excitations of a variety of 1D lattice systems in condensed matter and statistical mechanics. The theoretical and experimental interest of these systems has grown spectacularly in the last few years, due to the discovery of interesting and unexpected physical properties in spin chains and ladders.

The basic idea behind the MPM is the construction of the ground state and excitations of 1D or quasi-1D systems in a recursive way, by relating the states of the system with length N to that of length $N-1$. This simple idea has appeared in the past in different places. First of all, in the Wilson's real space renormalization group (RG) the 1D lattice is built up by the addition of a single site at every RG step [1]. This procedure is also used in the density matrix renormalization group method (DMRG) of White [2]. Another source of the MPM is the well known AKLT state of the spin 1 chain [3]. This is a simple but nontrivial example of a matrix product state, which has motivated various generalizations, see for example, Klümper *et al* [4], Ostlund and Rommer [5], etc. We shall follow the formulation of the MPM due to the latter authors, which is based on the analysis of the fixed point structure of the DMRG GS in the thermodynamic limit [5]. A closely related approach is that of Fannes *et al* [6]. The MPM offers an alternative formulation of the DMRG method in the regime where the latter reaches a fixed point after many RG iterations [7].

Whereas the DMRG is a purely numerical method, the MPM offers the possibility of an analytical approach to elucidate the actual structure of the GS and excitations. The MPM is

0305-4470/98/489729+31$19.50

a standard variational method which determines the variational parameters by minimizing the GS energy. Minimization problems are in general harder than diagonalization ones. In this respect the MPM is much less adequate than the DMRG. However, we believe that the analytical insights gained with the MPM could be used to boost the numerical precision and applications of both the MPM and the DMRG.

In this paper we apply the MPM to the two-legged spin ladder. Spin ladders with diagonal couplings have been studied with the MPM formulation of Klümper *et al* [4] in [8]. Spin ladders were first studied as theoretical laboratories to test ideas concerning the crossover from 1D to 2D, with the surprising result that this crossover is far from being smooth: the even and odd ladders display quite different properties converging only when the number of legs goes to infinity (for an introduction to the subject see [9]). Even spin ladders are spin liquids with a finite spin gap and finite spin correlation length, while odd spin ladders belong to the same universality class as the spin $\frac{1}{2}$ antiferromagnetic Heisenberg chain. This has no gap and its correlations decay algebraically. Another reason to study ladder systems is that materials actually exist with that structure and hence the theoretical predictions can, in principle, be compared with experimental data concerning the spectrum, susceptibility, etc.

In this paper we study five different spin ladders characterized by their local spin $S = \frac{1}{2}$, 1 and $\frac{3}{2}$ and the signs of the exchange of coupling constants along the legs $J_{\parallel}$ and the rungs $J_{\perp}$.

In the case of the spin $\frac{1}{2}$ ladders we discuss the following topics: (i) the resonating valence bond (RVB) picture of the antiferromagnetic ladder, (ii) the equivalence between the ladder state and the Haldane state of the spin 1 chain; and (iii) the duality properties relating the different magnetic structures.

In the case of the spin 1 ladder we show that the long-range topological order characteristic of isolated spin 1 chains disappears and the string correlator decays exponentially with a finite correlation length.

The study of the spin $\frac{3}{2}$ ladder motivates the definition of an AKLT state characterized in terms of 9-j symbols.

We compute GS energy densities, spin correlation lengths and string order parameters and compare our results with those in the current literature.

The organization of this paper is as follows. In section 2 we review the MPM. In section 3 we particularize the MPM to systems which are rotationally invariant, where the use of group theory leads to a simplification of the formalism. In section 4 we present our numerical results concerning five different spin ladders. In section 5 we summarize our results and present some prospects of our work. There are three appendices which contain technical details or proofs of results presented in the main body of the paper.

2. Review of the MPM

Some of the results presented in this section are already known and can be found in [5, 6]. We also present a full account of the formulae and derivations used in [7] where the MPM was compared with the DMRG method in the case of the antiferromagnetic spin 1 chain.

Let us consider a spin chain or a ladder B_N with open boundary conditions, where N denotes the number of sites of a chain or the number of rungs of a ladder. To describe the low-energy properties of B_N one introduces a collection of m states $\{|\alpha\rangle_N\}_{\alpha=1}^{m}$, which form an orthonormal basis, i.e. ${}_N\langle\alpha|\alpha'\rangle_N = \delta_{\alpha,\alpha'}$. In the DMRG these states are the most probable ones to contribute to the GS of the superblock $B_{N-1}\bullet\bullet B_{N-1}^{R}$ of length $2N$, formed

by adding two sites (or rungs) ••, and a mirror image B^R_{N-1} to the original lattice B_{N-1}. The basic assumption of the MPM is that the basis associated with B_N and B_{N-1} are related in a simple manner by the equation

$$|\alpha\rangle_N = \sum_{\beta,s} A_{\alpha,\beta}[s]|s\rangle_N \otimes |\beta\rangle_{N-1} \qquad N \geqslant 2 \tag{1}$$

where $|s\rangle_N (s = 1, \ldots, m^*)$ denotes a complete set of m^* states associated to the Nth site (resp. rung) added to the chain (resp. ladder). Equation (1) has to be supplemented with the initial data $|\beta\rangle_1$. The quantities $A_{\alpha,\beta}[s]$ are the variational parameters of the MPM, and their determination is the central problem one has to solve. This is done by the standard variational method. The important point about equation (1) is that $A_{\alpha,\beta}[s]$ does not depend on N. Equation (1) is motivated by the truncation method used in the DMRG where $A_{\alpha,\beta}[s]$ depends on N, i.e. $A^{(N)}_{\alpha,\beta}[s]$. When N is large enough one reaches a fixed point, i.e. $A^{(N)}_{\alpha,\beta}[s] \to A_{\alpha,\beta}[s]$. In this manner the thermodynamic limit of the DMRG leads to a translational invariant MPM state.

The condition that both $|\alpha\rangle_N$ and $|\beta\rangle_{N-1}$ form orthonormal basis imposes a normalization condition on $A_{\alpha,\beta}[s]$,

$$\sum_{\beta,s} A^*_{\alpha,\beta}[s]A_{\alpha',\beta}[s] = \delta_{\alpha,\alpha'}. \tag{2}$$

It is interesting to count how many variational parameters there are in (1). The quantities $A_{\alpha,\beta}[s]$ represent a total of m^2m^* variables. We shall assume that all of them may be nonvanishing. The normalization constraints (2) represent a total of $m + m(m-1)/2$ constraints (m coming from the diagonal terms $\alpha = \alpha'$ and $m(m-1)/2$ coming from the off-diagonal ones). On the other hand one can rotate the basis of states $\{|\alpha\rangle\}^m_{\alpha=1}$ by an element of the orthogonal group $O(m)$ reducing by $m(m-1)/2$ the number of independent MPM variables. The total number of variational degrees of freedom, N_A, is then given by,

$$N_A = m^2m^* - m - 2m(m-1)/2 = m^2(m^* - 1). \tag{3}$$

We show in appendix A that the set of $A_{\alpha,\beta}[s]$ belongs to the Grassmanian manifold:

$$A \in \frac{O(mm^*)}{O(m) \otimes O(m(m^* - 1))}. \tag{4}$$

As an exercise one can check that the dimension of (4) coincides with N_A given in (3).

In [5] equation (1) is used to generate an ansatz for the GS of periodic chains. In this paper we shall use this equation to generate states with open boundary conditions, in the spirit of the DMRG. We shall show below that the set $|\alpha\rangle$ corresponds to GSs with different boundary conditions. The use of open boundary conditions leads to a simplification of the MPM which is very close to the more abstract formalism proposed in [6].

2.1. Correlators of local operators

Let us use equation (1) to compute the expectation values of local operators in a recursive way. We shall first consider a local operator $\mathcal{O}_n$ acting at the position $n = 1, \ldots, N$ of the lattice. It is easy to get from (1) the expectation value,

$${}_N\langle\alpha|\mathcal{O}_n|\alpha'\rangle_N = \begin{cases} \displaystyle\sum_{\beta\beta'} T_{\alpha\alpha',\beta\beta'}{}_{N-1}\langle\beta|\mathcal{O}_n|\beta'\rangle_{N-1} & \text{for } n < N \\ \displaystyle\sum_{\beta} \hat{\mathcal{O}}_{\alpha\alpha',\beta\beta} & \text{for } n = N \end{cases} \tag{5}$$

where

$$T_{\alpha\alpha',\beta\beta'} = \sum_{s} A^{*}_{\alpha,\beta}[s]A_{\alpha',\beta'}[s] \tag{6}$$

$$\hat{\mathcal{O}}_{\alpha\alpha',\beta\beta'} = \sum_{ss'} A^{*}_{\alpha,\beta}[s]A_{\alpha',\beta'}[s']\langle s|\mathcal{O}|s'\rangle. \tag{7}$$

T can be identified with the operator $\hat{1}$ of [5]. Equations (5)–(7) suggest interpreting the expectation value ${}_N\langle\alpha|\mathcal{O}_n|\alpha'\rangle_N$ as a vector labelled by the pair $\alpha\alpha'$, in which case T and $\hat{\mathcal{O}}$ become $m^2 \times m^2$ matrices. Upon iteration of (5) one finds,

$${}_N\langle\alpha|\mathcal{O}_n|\alpha'\rangle_N = \sum_{\beta}(T^{N-n}\hat{\mathcal{O}})_{\alpha\alpha',\beta\beta}. \tag{8}$$

More generally, the expectation value of a product of local operators is given by,

$${}_N\langle\alpha|\mathcal{O}^{(1)}_{n_1}\mathcal{O}^{(2)}_{n_2}\dots\mathcal{O}^{(r)}_{n_r}|\alpha'\rangle_N = \sum_{\beta}(T^{N-n_1}\hat{\mathcal{O}}^{(1)}T^{n_1-n_2-1}\hat{\mathcal{O}}^{(2)}\dots T^{n_{r-1}-n_r-1}\hat{\mathcal{O}}^{(r)})_{\alpha\alpha',\beta\beta} \tag{9}$$

where $N \geqslant n_1 > n_2 > \cdots > n_r \geqslant 1$. The matrix T plays a very important role in the MPM. Equations (5), (9) imply that T behaves as a shift operator by one lattice space. The basic properties of T follow from the normalization condition (2) which can be expressed as

$$\sum_{\beta} T_{\alpha\alpha',\beta\beta} = \delta_{\alpha,\alpha'} \tag{10}$$

which implies that T has a eigenvalue equal to 1. Let us call $|v\rangle$ the right eigenvector corresponding to this eigenvalue. Equation (10) can be written in matrix notation as

$$T|v\rangle = |v\rangle \qquad v_{\alpha\alpha'} = \delta_{\alpha\alpha'}. \tag{11}$$

On the other hand, let $\langle\rho|$ denote the left eigenvector of T corresponding to the eigenvalue 1, i.e.

$$\langle\rho|T = \langle\rho| \leftrightarrow \sum_{\alpha\alpha'} \rho_{\alpha\alpha'}T_{\alpha\alpha',\beta\beta'} = \rho_{\beta\beta'}. \tag{12}$$

A convenient normalization of $\langle\rho|$ is given by

$$\langle\rho|v\rangle = 1 \leftrightarrow \sum_{\alpha} \rho_{\alpha\alpha} = 1. \tag{13}$$

For later use we shall diagonalize T as follows,

$$T = \sum_{p} x_p|v_p\rangle\langle\rho_p| \qquad \langle\rho_p|v_{p'}\rangle = \delta_{pp'} \tag{14}$$

where $|v_p\rangle$ and $\langle\rho_p|$ are the right and left eigenvectors of T with eigenvalue $x_p (x_1 = 1, |v_1\rangle = |v\rangle, \langle\rho_1| = \langle\rho|)$. As a matter of fact all the remaining eigenvalues of T are less than 1, i.e. $|x_p| < 1 \forall p \neq 1$.

In the limit $N \to \infty$ one gets,

$$\lim_{N\to\infty}\langle\alpha|\mathcal{O}^{(1)}_{n_1}\mathcal{O}^{(2)}_{n_2}\dots\mathcal{O}^{(r)}_{n_r}|\alpha'\rangle_N = \delta_{\alpha\alpha'}\langle\rho|\hat{\mathcal{O}}^{(1)}T^{n_1-n_2-1}\hat{\mathcal{O}}^{(2)}\dots T^{n_{r-1}-n_r-1}\hat{\mathcal{O}}^{(r)}|v\rangle. \tag{15}$$

The delta function on the r.h.s. of this equation means that the local operators $\hat{\mathcal{O}}^{(n)}$ acting in the bulk, do not modify the boundary conditions associated to the various choices of α.

Assuming that T is invertible, one can rewrite equation (15) in the following manner,

$$\lim_{N\to\infty_N}\langle\alpha|\mathcal{O}^{(1)}_{n_1}\mathcal{O}^{(2)}_{n_2}\dots\mathcal{O}^{(r)}_{n_r}|\alpha'\rangle_N = \delta_{\alpha\alpha'}\langle\rho|\tilde{\mathcal{O}}^{(1)}(n_1)\tilde{\mathcal{O}}^{(2)}(n_2)\dots\tilde{\mathcal{O}}^{(r)}(n_r)|v\rangle \tag{16}$$

where $\tilde{\mathcal{O}}(n)$ is defined as

$$\tilde{\mathcal{O}}(n) = T^{-n-1}\hat{\mathcal{O}}T^{n}. \tag{17}$$

Observe that $\tilde{1} = 1$. The r.h.s. of (16) is nothing but a spatial ordered product of local operators $\tilde{\mathcal{O}}(n)$, which is reminiscent of the radial ordered product that appears in conformal field theory. This connection supports the interpretation of T as an Euclidean version of the shift operator. Under this viewpoint the states $|v\rangle$ and $\langle\rho|$ appear as incoming $|0\rangle$ and outgoing vacua $\langle 0|$ that are left invariant by the shift operator T.

We have shown above that the MPM leads in the thermodynamic limit to a sort of discretized field theory characterized by a shift or spatial transfer operator T and local operators $\tilde{\mathcal{O}}(n)$. We can now try to exploit this interpretation to extract some physical quantities.

First of all let us consider the correlator of two operators $\mathcal{O}^{(1)}(n_1)$ and $\mathcal{O}^{(2)}(n_2)$. From (14), (15) one has,

$$\langle\rho|\hat{\mathcal{O}}^{(1)}T^{n_1-n_2-1}\hat{\mathcal{O}}^{(2)}|v\rangle = \sum_{p} x_p^{n_1-n_2-1}\langle\rho|\hat{\mathcal{O}}^{(1)}|v_p\rangle\langle\rho_p|\hat{\mathcal{O}}^{(2)}|v\rangle. \tag{18}$$

In the limit when $|n_1 - n_2| \gg 1$ the sum over p is dominated by the highest eigenvalue $|x_p|$ of T for which the corresponding matrix elements $\langle\rho|\hat{\mathcal{O}}^{(1)}|v_p\rangle$ and $\langle\rho_p|\hat{\mathcal{O}}^{(2)}|v\rangle$ are nonzero. If $x_p < 1$ one gets a finite correlation lenght ξ given by the formula,

$$\xi = -1/\ln|x_p|. \tag{19}$$

In the case where $\hat{\mathcal{O}}^{(1)}$ and $\hat{\mathcal{O}}^{(2)}$ are both the spin operator $\boldsymbol{S}$, it turns out that the matrix element $\langle\rho|\hat{\boldsymbol{S}}|v\rangle$ vanishes, and hence the spin–spin correlator is short ranged with a finite spin correlation length ξ given by the formula (19) with $|x_p| < 1$. The finiteness of ξ does indeed occur for MP ansätze which preserve the rotational invariance. If the latter is broken, as in a Neelstate, one can still find a finite value of ξ by studying the decay of the spin–spin correlator once the constant asymptotic value of the correlation is subtracted.

In section 3 we shall give a formula to compute ξ in the case of rotational invariant MP ansätzse.

Another interesting application of (16) is provided by the computation of the string order parameter.

2.2. String order parameter

A spin 1 chain has a long-range topological order (LRTO) characterized by a nonvanishing value of a nonlocal operator $g(\infty)$ defined as follows [10],

$$\begin{aligned} g(\infty) &= \lim_{\ell\to\infty} g(\ell) \\ g(\ell) &= \langle S^z(\ell)\prod_{k=1}^{\ell-1} \mathrm{e}^{\pi \mathrm{i} S^z(k)} S^z(0)\rangle. \end{aligned} \tag{20}$$

The AKLT state has $g_{\mathrm{AKLT}}(\infty) = -(\frac{2}{3})^2$, while the spin 1 antiferromagnetic spin chain has $g(\infty) = -0.374\,325$ [11]. From equation (15) we deduce the following expression for (20),

$$g(\ell) = \langle\rho|\widehat{S^z}(\widehat{\mathrm{e}^{\mathrm{i}\pi S^z}})^{\ell-1}\widehat{S^z}|v\rangle. \tag{21}$$

In appendix C we show that the operator $\widehat{\mathrm{e}^{\mathrm{i}\pi S^z}}$ has an eigenvalue equal to 1. Denoting by $|v^{\mathrm{st}}\rangle$ and $\langle\rho^{\mathrm{st}}|$ the associated right and left eigenvectors we obtain the following expression for the string order parameter

$$g(\infty) = \langle\rho|\widehat{S^z}|v^{\mathrm{st}}\rangle\langle\rho^{\mathrm{st}}|\widehat{S^z}|v\rangle \tag{22}$$

which suggests that $g(\infty)$ measures a sort of off-diagonal order.

For antiferromagnetic spin 1 ladders we shall see that the LRTO disappears and that the correlator (20) is short ranged with a finite correlation length ξ^{st}.

2.3. GS energy density

Let us suppose we have a translational invariant Hamiltonian of the form,

$$H_N = \sum_{n=1}^{N} h_n^{(1)} + \sum_{n=1}^{N-1} h_{n,n+1}^{(2)} \tag{23}$$

where $h^{(1)}$ is an on-site (rung) operator while $h^{(2)}$ couples two nearest-neighbour sites (rungs). We define the expectation value,

$$E_{\alpha\alpha'}^{N} =_N \langle\alpha|H_N|\alpha'\rangle_N \tag{24}$$

which can be computed recursively. From equations (1), (5) one gets

$$E_{\alpha\alpha'}^{N} = \sum_{\beta\beta'} T_{\alpha\alpha',\beta\beta'} E_{\beta\beta'}^{N-1} + \sum_{\beta} \hat{h}_{\alpha\alpha',\beta\beta} \qquad (N \geqslant 2) \tag{25}$$

where $\hat{h} = \hat{h}^{(1)} + \hat{h}^{(2)}$. The hated representation of the site Hamiltonian $h^{(1)}$ is given by equation (7), while the hated representation of the Hamiltonian $h^{(2)}$ is given by,

$$\hat{h}^{(2)}_{\alpha\alpha',\beta\beta'} = \sum_{\gamma\gamma' s' s} {}_{N-1,N}\langle s_2 s_1|h^{(2)}_{N-1,N}|s_1' s_2'\rangle_{N,N-1} A^*_{\alpha,\gamma}[s_1] A^*_{\gamma,\beta}[s_2] A_{\alpha',\gamma'}[s_1'] A_{\gamma',\beta'}[s_2']. \tag{26}$$

It should be clear from equations (7), (26) which is the hated representative of an operator involving an arbitrary number of sites. Equation (25) can be conveniently written in matrix notation as

$$|E^N\rangle = T|E^{N-1}\rangle + \hat{h}|v\rangle \qquad (N \geqslant 2) \tag{27}$$

where $|E^N\rangle$ is a vector with components $E^N_{\alpha\alpha'}$. Iterating (27) one gets

$$|E^N\rangle = (1 + T + T^2 + \cdots + T^{N-2})\hat{h}|v\rangle + T^{N-1}|E^1\rangle. \tag{28}$$

The geometric series in T can be sumed up and due to the eigenvalue equal to 1 it contributes a term proportional to N, i.e.

$$\lim_{N\to\infty} \frac{1}{N}|E^N\rangle = e_\infty|v\rangle. \tag{29}$$

This equation implies that all the states $|\alpha\rangle_N$ have the same energy density in the thermodynamic limit, i.e. $E^N_{\alpha\alpha'} = \delta_{\alpha\alpha'} e_\infty$. Hence e_∞ can be identified with the GS energy per site for chains or per rung for ladders and it is given by,

$$e_\infty = \langle\rho|\hat{h}|v\rangle = \sum_{\alpha\alpha'\beta} \rho_{\alpha\alpha'} \hat{h}_{\alpha\alpha',\beta\beta}. \tag{30}$$

This is the quantity one has to minimize with respect to the MPM parameters.

The formalism presented above is closely related to the DMRG. Even though this relation is not the main subject of this paper we shall make some remarks (see [7]).

2.4. MPM versus the DMRG

Let us suppose that we diagonalize ρ, as a $m \times m$ matrix, denoting its eigenvalues as w_α^2, i.e.

$$\rho_{\alpha\alpha'} = w_\alpha^2 \delta_{\alpha\alpha'}. \tag{31}$$

The eigenvalue equation (12) then becomes,

$$\sum_{\alpha s} w_\alpha^2 A_{\alpha\beta}[s] A^*_{\alpha\beta'}[s] = \delta_{\beta\beta'} w_\beta^2. \tag{32}$$

There is a close analogy between equations (2) and (32), except for the fact that the order of the labels is exchanged. Given the tensor product decomposition $s \otimes \beta \to \alpha$, we shall assume that one can reverse the order between the states α and β in terms of 'charge conjugate states' α^c and β^c, as follows: $s \otimes \alpha^c \to \beta^c$. For example, the charge conjugate of a state with spin M is another state with spin $-M$. Using this concept we can impose the following symmetry condition [12],

$$w_\alpha A_{\alpha\beta}[s] = \pm w_{\beta^c} A_{\beta^c\alpha^c}[s] \qquad w_{\beta^c} = w_\beta \tag{33}$$

which leads to the equivalence between equations (2) and (32).

The relation between the MPM and the DMRG is made clear by the construction of the GS of the superblock $B_N \bullet B_N^R$ in the following way:

$$|\psi_0\rangle = \sum \psi_{\alpha s\beta} |\alpha^R\rangle \otimes |s\rangle \otimes |\beta\rangle \psi_{\alpha s\beta} = w_\alpha A_{\alpha\beta}[s]. \tag{34}$$

The density matrix that induces $\psi_{\alpha s\beta}$ on the block B_N, and which is obtained by tracing over the states in $\bullet B_N^R$, coincides with $\rho_{\alpha\alpha'} = w_\alpha^2 \delta_{\alpha\alpha'}$.

Condition (33) guarantees that $|\psi_0\rangle$ is a state invariant under the parity transformation that interchanges the blocks B_N and B_N^R, while leaving invariant the site $\bullet$.

It is interesting to observe that the MPM leads to a superblock of the form $B_N \bullet B_N^R$, rather than to the standard superblock $B_N \bullet \bullet B_N^R$ [7].

3. The MPM applied to spin ladders

In this section we shall apply the MPM to the two-legged spin ladder with a spin S at each site of the chain. The collection $|\alpha\rangle_N$ will be given by the set $|JM\rangle_N (J \leqslant J_{\max})$ of states with total spin J and third component M. For the sake of simplicity we have only considered one state per angular momenta J and M. This will allow us to show more clearly the analytic structure of the MPM, which can later be numerically improved upon by considering multiplicity. This has already been done in the case of spin chains in [5, 7].

The states added at each step of the MPM are the ones that appear in the tensor product decomposition of two spin S irreps, i.e. $S \otimes S = 0 \oplus 1 \oplus \cdots \oplus 2S$. These states are labelled by $|\lambda\mu\rangle$ where $\lambda = 0, \ldots, 2S$ is the total spin and $\mu = -\lambda, \ldots, \lambda$ is its third component.

Using these notations we propose the following recurrence relation for the states $|JM\rangle_N$,

$$|J_1 M_1\rangle_N = \sum_{\lambda J_2} A^\lambda_{J_1 J_2} |(\lambda J_2), J_1 M_1\rangle_N \tag{35}$$

where

$$|(\lambda J_2), J_1 M_1\rangle_N = \sum_\mu \langle \lambda\mu, J_2 M_2 | \lambda J_2, J_1 M_1\rangle |\lambda\mu\rangle_N \otimes |J_2 M_2\rangle_{N-1}. \tag{36}$$

In (36) the quantity $\langle \lambda\mu, J_2 M_2 | \lambda J_2, J_1 M_1\rangle$ is the Clebsch–Gordan (CG) coefficient corresponding to the decomposition $\lambda \otimes J_2 \to J_1$. Comparing equations (1) and (35)

we obtain the following relation between the symbols $A_{J_1M_1,J_2M_2}[\lambda\mu]$ and the rotational invariant symbols $A^{\lambda}_{J_1J_2}$,

$$A_{J_1M_1,J_2M_2}[\lambda\mu] = A^{\lambda}_{J_1J_2}\langle\lambda\mu,\, J_2M_2|\lambda J_2,\, J_1M_1\rangle. \tag{37}$$

The use of the rotational invariant basis considerably reduces the number of independent variational parameters and consequently increases the power of the MPM [5, 7].

The variational parameters $A^{\lambda}_{J_1J_2}$ are subject to the CG condition,

$$A^{\lambda}_{J_1J_2} = 0 \text{ unless } |\lambda - J_2| \leqslant J_1 \leqslant |\lambda + J_2|. \tag{38}$$

Using (37) and the orthogonality properties of the CG coefficients, the normalization conditions (2) become,

$$\sum_{\lambda,J_2} |A^{\lambda}_{J_1J_2}|^2 = 1 \qquad \forall J_1. \tag{39}$$

At this point we can just take equation (37) and plug it into the corresponding formulae of section 2 in order to derive expectation values, the GS energy density, etc in terms of $A^{\lambda}_{J_1J_2}$. There is, however, a more efficient way to do this by using group theory. The application of the Wigner–Eckart theorem will allow us to express all the results in terms of reduced matrix elements of the operators involved as well as the 6-j symbols. In our derivations we shall follow the same steps as in section 2, leaving the technical details to appendix B.

3.1. Correlators of invariant tensors

Let us denote by $\mathcal{O}^{(k)}$ an irreducible tensor of total angular momentum k, whose components are labelled by $\mathcal{O}^{(k)}_M$, $M = -k, \ldots, k$. The spin operators $\boldsymbol{S}$ correspond to $k = 1$. Let us suppose we have two irreducible tensors with the same total angular momenta k, $\mathcal{O}^{(k,A)}(n)$ and $\mathcal{O}^{(k,B)}(m)$, acting at the positions n and m ($N \geqslant n > m \geqslant 1$) of the ladder. The scalar product of these two operators is defined as

$$\mathcal{O}^{(k,A)}(n)\cdot\mathcal{O}^{(k,B)}(m) = \sum_{M=-k}^{k} (-1)^{-M}\mathcal{O}^{(k,A)}_{M}(n)\cdot\mathcal{O}^{(k,B)}_{-M}(m). \tag{40}$$

The basic result we derive in appendix B is,

$${}_N\langle J_1M|\mathcal{O}^{(k,A)}(n)\cdot\mathcal{O}^{(k,B)}(m)|J_1M\rangle_N = \sum_{J_2,\ldots,J_7} T^{N-n}_{J_1J_2}\hat{\mathcal{O}}^{(k,A)}_{J_2,J_3J_4}(T^{n-m-1}_{k})_{J_3J_4,J_5J_6}\hat{\mathcal{O}}^{(k,B)}_{J_5J_6,J_7} \tag{41}$$

where T and $T^{(k)}$ are defined as,

$$T_{J_1,J_2} = \sum_{\lambda}(A^{\lambda}_{J_1J_2})^{*}A^{\lambda}_{J_1J_2} \tag{42}$$

$$(T_k)_{J_1J_2,J_3J_4} = \sum_{\lambda}(A^{\lambda}_{J_1J_3})^{*}A^{\lambda}_{J_2J_4}(-1)^{\lambda+k+J_1+J_4}\sqrt{(2J_1+1)(2J_2+1)}\begin{Bmatrix} J_3 & J_1 & \lambda \\ J_2 & J_4 & k \end{Bmatrix} \tag{43}$$

while $\hat{\mathcal{O}}^{(k,B)}$ and $\hat{\mathcal{O}}^{(k,B)}$ are defined in appendix B.

Equation (41) is the invariant version of (9) involving only two operators. In order to obtain the thermodynamic properties of (41) we use the properties of the transfer operator T. The normalization conditions (39) imply the following conditions on T,

$$\sum_{J_2} T_{J_1,J_2} = 1 \qquad \forall J_1. \tag{44}$$

Let us call ρ_J the left eigenvector of T_{J_1,J_2} with eigenvalue 1, i.e.

$$\sum_{J_1} \rho_{J_1} T_{J_1,J_2} = \rho_{J_2}. \tag{45}$$

Using equations (44), (45) into (41) and taking $N \gg 1$ we get

$$\lim_{N\to\infty} {}_N\langle J_1 M|\mathcal{O}^{(k,A)}(n)\cdot\mathcal{O}^{(k,B)}(m)|J_1 M\rangle_N = \langle\rho|\hat{\mathcal{O}}^{(k,A)} T_k^{n-m-1}\hat{\mathcal{O}}^{(k,B)}|v\rangle \tag{46}$$

where we use a matrix notation in J-space with the convention $v_J = 1, \forall J$. From equation (46) we deduce that the correlation length associated to the scalar product of two irreducible operators with angular momentum k, is given by the highest eigenvalue of the matrix T_k defined in (43). The spin–spin correlation length is obtained by looking at the highest absolute eigenvalue of T_1.

3.2. GS energy density

The Hamiltonian of the two-legged ladder has the form proposed in (23) where $h^{(1)}$ is the rung Hamiltonian and $h^{(2)}$ is the leg Hamiltonian,

$$h_n^{(1)} = J_\perp \boldsymbol{S}_1(n)\cdot\boldsymbol{S}_2(n) \tag{47}$$

$$h_{n,n+1}^{(2)} = J_\parallel(\boldsymbol{S}_1(n)\cdot\boldsymbol{S}_1(n+1) + \boldsymbol{S}_2(n)\cdot\boldsymbol{S}_2(n+1)) \tag{48}$$

$\boldsymbol{S}_a(n)$ is a spin S operator acting on the $n = 1,\ldots,N$ rung and the $a = 1,2$ leg of the ladder.

As in (24) we define the expectation value of the ladder Hamiltonian,

$$E_J^N =_N \langle JM|H_N|JM\rangle_N. \tag{49}$$

Using (35) we find

$$E_{J_1}^N = \sum_{J_2}(T_{J_1,J_2}E_{J_2}^{N-1} + \hat{h}_{J_1,J_2}) \qquad (N \geqslant 2) \tag{50}$$

where $\hat{h} = \hat{h}^{(1)} + \hat{h}^{(2)}$ ($\hat{h}^{(1)}$ and $\hat{h}^{(2)}$ can be found in appendix B).

Iterating equation (50) and using the properties of the matrix T we can immediately get the large N limit of the energy (49),

$$\lim_{N\to\infty}\frac{1}{N}E_J^N = e_\infty \qquad \forall J \tag{51}$$

where the GS energy density is given by,

$$e_\infty = \langle\rho|\hat{h}|v\rangle = \sum_{J_1,J_2}\rho_{J_1}\hat{h}_{J_1J_2}. \tag{52}$$

At this point let us summarize the main steps of the MP algorithm hereby proposed.

- Solve the normalization conditions (39) expressing $A^\lambda_{J_1J_2}$ in terms of a set of linearly independent variational parameters.
- Find the eigenvector ρ_J of the matrix T.
- Minimize the GS energy density (52) with respect to the independent variational parameters.

We will now comment on how these three steps can be implemented.

3.3. Solution of the normalization conditions

We shall suppose in the rest of the paper that the parameters $A^{\lambda}_{J_1J_2}$ are all real. Hence the normalization conditions

$$\sum_{\lambda,J_2}(A^{\lambda}_{J_1J_2})^2 = 1 \qquad \forall J_1 \tag{53}$$

imply that the set $\{A^{\lambda}_{J_1J_2}\}$ for J_1 fixed are the coordinates of a sphere whose dimension depends on the allowed values of J and the CG conditions (38). Let us call $A^{\max}_{J_1}$ the highest coordinate, in absolute value, i.e.

$$A^{\max}_{J_1} = A^{\lambda_0}_{J_1L_0} \text{ such that } |A^{\lambda_0}_{J_1L_0}| \geqslant |A^{\lambda}_{J_1J_2}| \forall \lambda, J_2. \tag{54}$$

If $A^{\max}_{J_1} > 0$ (resp. $A^{\max}_{J_1} < 0$) we can think of it as the north (resp. south) pole of a sphere, whose neighbourhood can be described by the stereographic coordinates,

$$x^{\lambda}_{J_1J_2} = A^{\lambda}_{J_1J_2}/A^{\max}_{J_1} \qquad |x^{\lambda}_{J_1J_2}| \leqslant 1. \tag{55}$$

Note that $x^{\lambda_0}_{J_1L_0} = 1$. The remaining coordinates are the independent variational parameters used in the minimization of the GS energy. The solution of the constraint (53) finally reads,

$$A^{\lambda}_{J_1J_2} = \epsilon_{J_1}x^{\lambda}_{J_1J_2}\left(\sum_{\lambda',J_2'}(x^{\lambda'}_{J_1J_2'})^2\right)^{-1/2} \qquad \epsilon_J = \pm 1 \tag{56}$$

where $\epsilon_{J_1} = 1(-1)$ corresponding to the north (south) pole of the above-mentioned sphere.

3.4. Determination of ρ_J

The solution of the eigenvalue problem of equation (45) can be done numerically. However, for a ladder with spin $S = \frac{1}{2}$ it can also be solved analytically which will allow us to make some considerations on the nature of ρ_J. In the case where $S = \frac{1}{2}$ the allowed values for λ are 0 and 1. Hence the unique nonvanishing entries of $A^{\lambda}_{J_1J_2}$ are A^0_{JJ}, A^1_{JJ}, A^1_{JJ+1} and A^1_{JJ-1}. Similarly from equation (42) the nonvanishing entries of T are $T_{J,J}$, $T_{J,J+1}$ and $T_{J,J-1}$. The set of equations we therefore have to solve read explicitly as,

$$\begin{aligned} &T_{J,J} + T_{J,J+1} + T_{J,J-1} = 1 \\ &\rho_J T_{J,J} + \rho_{J+1}T_{J+1,J} + \rho_{J-1}T_{J-1,J} = \rho_J \\ &\sum_{J=0}^{J_{\max}}\rho_j = 1. \end{aligned} \tag{57}$$

The solution of these equations is given by

$$\rho_J = \frac{u_J}{\sum_L u_L} \tag{58}$$

where

$$u_0 = 1 \qquad u_J = \prod_{L=0}^{J}\frac{T_{L,L+1}}{T_{L+1,L}}(J > 0) \tag{59}$$

we are assuming that $J = 0, \ldots, J_{\max}$.

Equations (58), (59) imply that ρ_J is always positive, in agreement with the Perron–Frobenius theorem applied to the matrix T, whose entries are all non-negative. In [7] it was shown that the values of ρ_J are intimately related to the eigenvalues of the density matrix

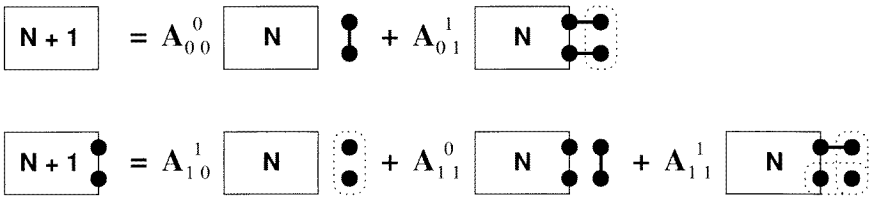

Figure 1. Graphical representation of the MP ansatz (35) in the case of the spin $\frac{1}{2}$ ladder and basis $|JM\rangle_N$ with $J = 0$ and 1. Each dot represents a spin $\frac{1}{2}$. A link between two dots denotes the formation of a singlet between the spins. Dotted lines denote symmetrization of the spins encircled by them.

that appear in the DMRG. These and other facts suggest that the MPM is in fact equivalent to the DMRG, especially when the number of states kept m becomes large.

This completes the presentation of the formalism.

4. Numerical results

In this section we shall apply the MPM to five different spin ladders, corresponding to different choices of the spin S and signs of the coupling constants $J_\parallel$ and $J_\perp$. We shall denote every of these ladders as AA_S, AF_S, and FA_S, where A and F stands for antiferromagnetic or ferromagnetic couplings. Thus, for example, AF_S is a spin S ladder with antiferromagnetic couplings along the legs and ferromagnetic couplings along the rungs. With these notations we will study below the following cases: $AA_{1/2}$, $AF_{1/2}$, $FA_{1/2}$, AA_1 and $AA_{3/2}$. Within each case we will highlight a particular aspect, which the MPM helps to clarify.

4.1. $AA_{1/2}$ ladder: the dimer-RVB state

This is the most studied spin ladder. Its properties are well known and can be summarized as follows. In the weak coupling regime, i.e. $J_\perp \ll J_\parallel$, the gapless spin $\frac{1}{2}$ chains become massive by the interchain coupling which is a relevant operator of dimension one [13–15]. The magnitude of the gap is proportional to $J_\perp$. In the intermediate coupling regime, i.e. $J_\perp \simeq J_\parallel$ the spin ladder can be mapped into the $O(3)$ nonlinear sigma model (NLSM) with no topological term [16–18]. This model is known to have a spin gap. From numerical studies the magnitude of the spin gap Δ and the spin correlation length, in the isotropic case $J_\perp = J_\parallel = J$, are given by $\Delta = 0.502J$ and $\xi = 3.2$ respectively [19–22]. In the strong coupling regime $J_\perp \gg J_\parallel$, the most appropiate physical picture of the GS and excitations is given by the RVB scenario proposed in [20], and supported by DMRG [20], mean field [23] and variational calculations [24]. In the latter work a recurrent variational ansatz (RVA) was proposed to generate the dimer-RVB and generalizations of it. The RVA method is a MPM based on second- and higher-order recurrent relations, while the standard MPM is based on a first-order relation. We shall see below that the MPM applied to ladders essentially contains the RVA, and that the numerical results are improved.

Let us first consider the case where the MPM states $|JM\rangle_N$ are choosen to be a singlet and a triplet, i.e. $J = 0$ and 1. In this case equation (35) is depicted in figure 1. There are *a priori* five nonvanishing MP parameters subjected to two normalization constraints, leaving a total of three independent parameters.

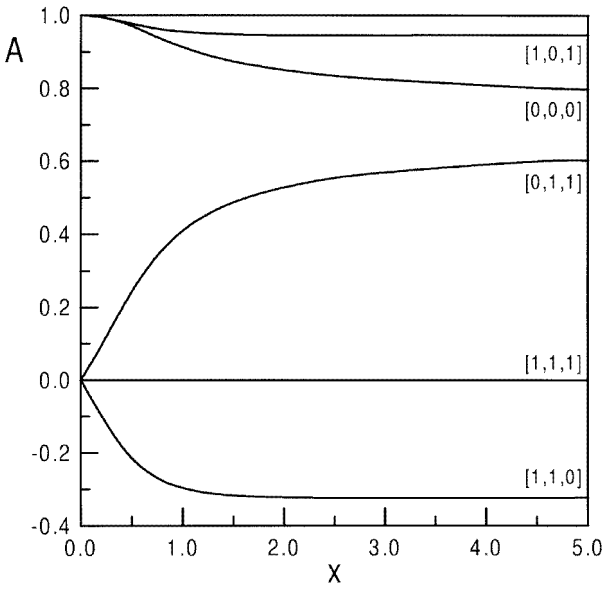

Figure 2. The MP parameters for the ladder $AA_{1/2}$. In figures 2–10 we adopt the notation $x = |J_\parallel/J_\perp|$. The curve $A^{\lambda}_{J_1 J_2}$ is labelled as $[J_1, J_2, \lambda]$.

Table 1. GS energy per site $-e_\infty/2J_\perp$ of the ladder $AA_{1/2}$. The first two columns are the MPM results. The RVA results are obtained with a third-order recursion formula [24]. The mean field and Lanczos results have been obtained in [23, 25] respectively.

$J_\parallel/J_\perp$	$J_{\max} = 1$	$J_{\max} = 2$	RVA	Mean field	Lanczos
0.0	0.375 000	0.375 000	0.375 000	0.375 000	
0.2	0.383 199	0.383 199	0.383 195	0.382 548	
0.4	0.409 607	0.409 608	0.409 442	0.405 430	
0.6	0.453 509	0.453 513	0.452 52	0.442 424	
0.8	0.510 504	0.510 523	0.507 909	0.489 552	
1.0	0.575 924	0.575 970	0.571 314	0.542 848	0.578
1.25	0.664 776	0.664 867	0.657 551	0.614 473	0.6687
1.66	0.819 656	0.819 834	0.808 438	0.738 360	0.8333
2.5	1.152 056	1.152 416	1.133 84	1.002856	1.18
5.0	2.172 002	2.172 878	2.136 08		2.265

Figure 2 shows $A^{\lambda}_{J_1 J_2}$ as functions of $x = J_\parallel/J_\perp$. In the whole range of coupling constants the most important amplitudes are A^0_{00} and A^1_{10} while A^1_{11} is essentially zero. The latter amplitude corresponds to having only a single bond among two rungs (see figure 1), which is forbidden in the dimer-RVB picture of [20, 24].

In table 1 we show the GS energy density obtained with the MPM for $J_{\max} = 1$ and 2, together with the RVA, mean field and Lanczos results. In table 2 we give the spin correlation length computed with the MPM and the RVA.

There is an appreciable improvement in the numerical results of the MPM respect to the RVA, especially for the spin correlation length. However, the later quantity is still understimated by the MPM since its exact value for $J_\perp = J_\parallel$ is given by $\xi = 3.2$ [19–22], while we get $\xi \sim 1.4$ for $J_{\max} = 1$ and 2. This shows that in order to improve the value

Table 2. Spin correlation length of the ladder $AA_{1/2}$. The first two columns are the MPM results. The RVA results are those of [24].

$J_\parallel/J_\perp$	$J_{\max}=1$	$J_{\max}=2$	RVA
0.0	0.00000	0.0000	0.000 000
0.2	0.5300	0.5303	0.437 166
0.4	0.8057	0.8081	0.608 323
0.6	1.0652	1.0740	0.751 286
0.8	1.2753	1.2945	0.866 958
1.0	1.4282	1.4593	0.959 249
1.25	1.5572	1.6018	1.048 77
1.66	1.6802	1.7413	1.152 05
2.5	1.7903	1.8698	1.269 51
5.0	1.8747	1.9711	1.385 32

of ξ one should consider a MPM built in with several states for fixed values of J as is the case of the spin 1 chain [5, 7]. Multiplicity seems to be a key ingredient of the DMRG method which the MPM should also incorporate in order to achieve exactness.

4.2. $AF_{1/2}$ ladder: relation with the spin 1 chain

The ladder with magnetic structure AF is interesting because it is intimately related to the spin 1 chain [26]. This relation can be clearly seen in the strong coupling limit $-J_\perp \gg J_\parallel$, since it leads to an effective spin 1 on every rung, which are effectively coupled antiferromagnetically along the legs. The effective Hamiltonian can be derived from (47), (48) and reads [26],

$$H_{\rm eff}^{\rm ladder} = -\tfrac{1}{4}|J_\perp|N + \tfrac{1}{2}J_\parallel \sum_n \boldsymbol{S}_{\rm eff}\cdot\boldsymbol{S}_{\rm eff} \tag{60}$$

where $\boldsymbol{S}_{\rm eff}(n) = \boldsymbol{S}_1(n) + \boldsymbol{S}_2(n)$ is the spin 1 operator acting on the nth rung. The term proportional to $J_\perp$ comes from the rung Hamiltonian when diagonalized in the spin 1 sector. This equation implies the following relation between the energy per site of the AF ladder, e_∞^{AF}, and the energy per site of the effective spin 1 chain, $e^{\rm eff}$,

$$e_\infty^{AF} = -\tfrac{1}{8}|J_\perp| + \tfrac{1}{4}J_\parallel e_\infty^{\rm eff}. \tag{61}$$

The energy density of the spin 1 chain is known to great accuracy from the DMRG and it is given by $e_\infty = -1.401\,4845$ [11]. From this result and using equation (61) we can compute the GS energy density of the ladder for different values of $J_\perp$ and $J_\parallel$ and compare the corresponding results with the ones obtained with the MPM. If we choose a MPM with $J = \frac{1}{2}$ and $\frac{3}{2}$ then the GS energy density in the range $0 < -J_\parallel/J_\perp < 5$ is given by equation (61) with $e_\infty^{\rm eff} = -1.399\,659$. The last value is pretty close to the expected $-1.401\,4845$, which indeed supports the validy of the mapping (60) in the region $|J_\parallel/J_\perp| < 5$. On the other hand the spin correlation length of our MPM ansatz is $\xi_{\rm ladder} = 2.6$ which is to be compared with the corresponding value for the spin chain $\xi_{\rm chain} = 6.03$ [11]. The MPM again understimates the value of ξ. Our results provide additional support for the equivalence between the $AF_{1/2}$ ladder and the antiferromagnetic spin 1 chain in the strong and intermediate coupling regimes in agreement with other authors [26].

Table 3. GS energy per site and correlation length of the ladder $FA_{1/2}$.

$-J_{\parallel}/J_{\perp}$	$-e_{\infty}/2J_{\perp}$	ξ
0.0	0.375 000	0.0000
0.2	0.381 754	0.5140
0.4	0.399 295	0.7577
0.6	0.424 396	1.010
0.8	0.454 891	1.277
1.0	0.489 324	1.554
1.25	0.536 374	1.895
1.66	0.619 895	2.381
2.5	0.803 434	2.992
5.0	1.376 973	3.520

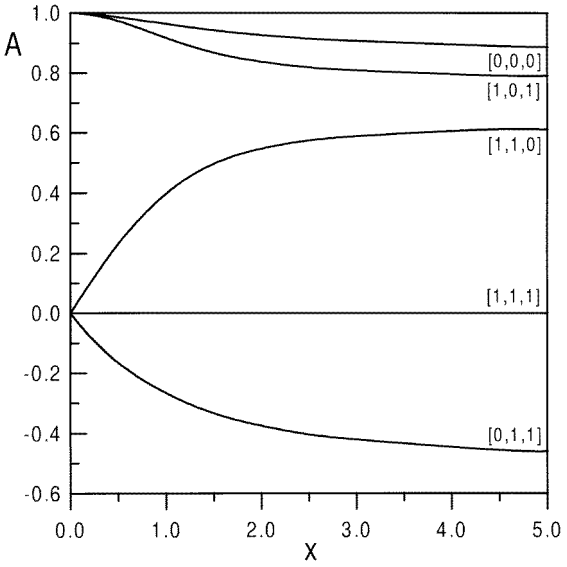

Figure 3. The MP parameters for the $FA_{1/2}$ ladder. We follow the same conventions as in figure 2.

4.3. $FA_{1/2}$ ladder

In the strong coupling regime the ladders $FA_{1/2}$ and $AF_{1/2}$ have similar GS energies and correlation lengths (see tables 1–3). The MP parameters also display a similar behaviour, although some of them are interchanged (see figures 2 and 3). The physical reason for this is the common GS in the case where $J_{\parallel} = 0$, given by the coherent superposition of valence bonds in the rungs.

The relation between $FA_{1/2}$ and $AF_{1/2}$ is part of a more general relation also involving the ladder $AA_{1/2}$ and can be established by types of transformations called dualities in [29].

4.4. Duality properties of spin ladders

On a two-legged ladder one can define three types of dualities called U, T and S, which mix or leave invariant the ladder's magnetic structures AA, AF and FA [29]. These

Table 4. Dictionary establishing the correspondences between concepts defined on a torus and on spin ladders [29].

Torus	Spin ladder
a-cycle	legs
b-cycle	rungs
periodic BC	ferromagnetic coupling
antiperiodic BC	antiferromagnetic coupling
modular transformation	bond transformation

transformations are discrete analogues of the modular transformations that mix different spin structures of the fermions defined on a surface with the topology of a torus. We recall that a spin structure specifies the periodic or antiperiodic boundary conditions (BC) of a fermion along a cycle. There is a dictionary that relates the spin ladder case to the torus case which is given in table 4 by [29],

A fermion on a torus has four possible spin structures labelled as AA, AP, PA and PP, where for example, AP means that the corresponding fermion is antiperiodic along the a-cycle but periodic along the b-cycle. The modular transformations T, U and S have the effect of mixing or leaving invariant the spin structures AA, AP and PA, while the spin structure PP is left invariant under all the modular transformations [30]:

$$\begin{aligned} &T : AA \leftrightarrow AP \qquad PA \leftrightarrow PA, PP \leftrightarrow PP \\ &U : AA \leftrightarrow PA \qquad AP \leftrightarrow AP, PP \leftrightarrow PP \\ &SAP \leftrightarrow PA \qquad AA \leftrightarrow AA, PP \leftrightarrow PP. \end{aligned} \tag{62}$$

Equations (62) can be proved by using the modular properties of the theta functions [30].

In [29] it was shown, using bosonization, perturbation theory and the nonlinear sigma model, that the spin ladders with magnetic structures AA, AF and FA can be related by equations similar to (62) under the translation provided by table 4, by a discrete analogue of the modular transformations of the torus. The case FF is trivial since the GS is simply the fully polarized state which is left invariant under all the modular transformations, just like the fermion with PP boundary conditions.

In this section we shall use the MPM to give further evidence for the duality or modular properties of the spin ladders.

In the case of the torus the modular properties reflect the essential equivalence of the fermions with different spin structures. In the case of the ladder the duality properties also reflect the fact that the GS obtained with different choices of the signs of the exchange coupling constants is essentially equivalent and suggests that this equivalence has possibly a deep geometrical and/or topological origin.

Let us come now to our results. We refer to [29] for the proof of the basic equations presented below. The U duality maps a Hamiltonian with couplings constants $J_\parallel, J_\perp$ into a ladder with couplings constants $J_\parallel^U, J_\perp^U$ where

$$\begin{aligned} J_\parallel^U &= J_\parallel \langle \boldsymbol{S}_1(n) \cdot \boldsymbol{S}_1(n+1) \rangle / \langle \boldsymbol{S}_1(n) \cdot \boldsymbol{S}_2(n+1) \rangle \\ J_\perp^U &= J_\perp. \end{aligned} \tag{63}$$

Under U the leg-bonds are transformed into diagonal ones while the rung-bonds are left invariant. The signs of $\langle \boldsymbol{S}_1(n) \cdot \boldsymbol{S}_1(n+1) \rangle$ and $\langle \boldsymbol{S}_1(n) \cdot \boldsymbol{S}_2(n+1) \rangle$ are determined by those

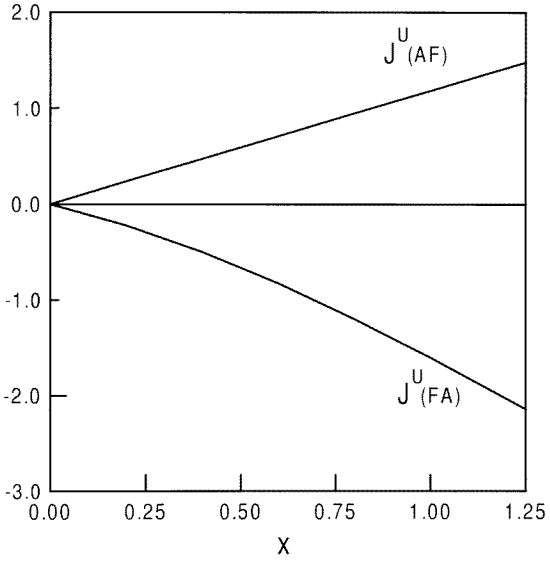

Figure 4. Graphical representation of $J^U(AF) \equiv J_\parallel^U(AF)$ and $J^U(FA) \equiv J_\parallel^U(FA)$ as computed using equations (63).

of $J_\parallel$ and $J_\perp$ respectively. Thus U acts on the magnetic structures as follows:

$$\begin{aligned} &AA \xrightarrow{U} FA \\ &J_\parallel(AA) > 0 \rightarrow J_\parallel^U(FA) < 0 \\ &J_\perp(AA) > 0 \rightarrow J_\perp^U(FA) > 0 \end{aligned} \tag{64}$$

$$\begin{aligned} &AF \xrightarrow{U} AF \\ &J_\parallel(AF) > 0 \rightarrow J_\parallel^U(AF) > 0 \\ &J_\perp(AF) < 0 \rightarrow J_\perp^U(AF) < 0 \end{aligned} \tag{65}$$

in agreement with equations (62) when properly translated into magnetic language. In figure 4 we show $J_\parallel^U(FA)$ and $J_\parallel^U(AF)$ as functions of $J_\parallel(AA)$ and $J_\parallel(AF)$, respectively.

As shown in [29] the GS energy density of the ladder with coupling constants $J_\parallel^U$, $J_\perp^U$ is a lower bound of the original GS energy,

$$\begin{aligned} &e_\infty(J_\parallel^U(FA), J_\perp^U(FA)) \leqslant e_\infty(J_\parallel(AA), J_\perp(AA)) \\ &e_\infty(J_\parallel^U(AF), J_\perp^U(AF)) \leqslant e_\infty(J_\parallel(AF), J_\perp(AF)). \end{aligned} \tag{66}$$

In figure 5 we show the validity of these inequalities, which in the strong coupling limit almost become identities. In figure 6 we show the correlation lengths for both AA and the transformed FA ladders. Figures 5 and 6 show that in the strong coupling regime the ladders AA and FA are U-dual while the ladder AF is self-U-dual.

The T transformation consists in the replacement of the vertical bonds by diagonal ones, which leads to

$$\begin{aligned} &J_\parallel^T = J_\parallel \\ &J_\perp^T = J_\perp \langle \boldsymbol{S}_1(n) \cdot \boldsymbol{S}_1(n+1) \rangle / \langle \boldsymbol{S}_1(n) \cdot \boldsymbol{S}_2(n+1) \rangle. \end{aligned} \tag{67}$$

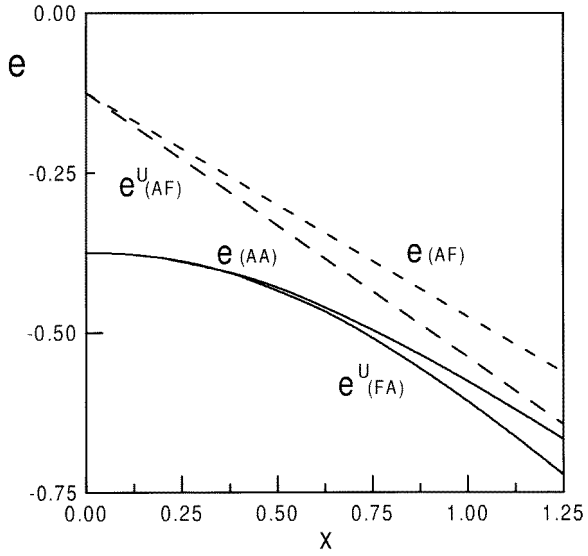

Figure 5. GS energy per site of the AA and AF ladders and their U-dual models. Observe that the inequalities (66) are indeed satisfied.

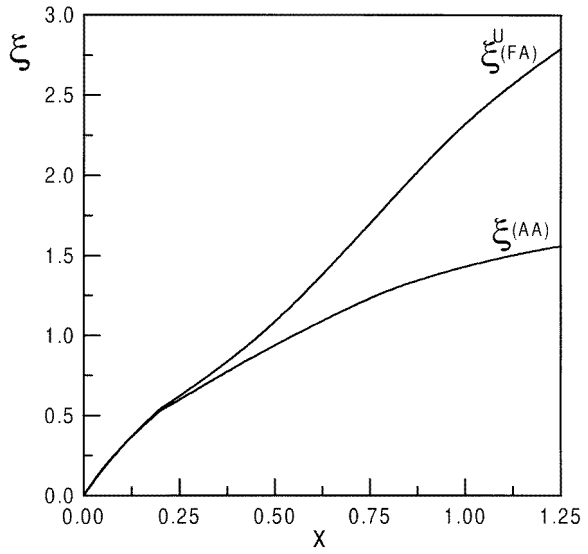

Figure 6. Spin correlation lengths of the AA ladder and its U dual.

In figure 7 we plot the energies associated to the FA ladder and its T transformed, which satisfies the inequality,

$$e_\infty(J_\parallel^T(FA), J_\perp^T(FA)) \leqslant e_\infty(J_\parallel(FA), J_\perp(FA)). \tag{68}$$

The convergence of both curves in the weak coupling together with the bosonization arguments employed in [29] allow us to conclude that in the weak coupling regime the FA ladder is self-T-dual while AA and AF ladders are T-dual in agreement with the magnetic analogue of (62).

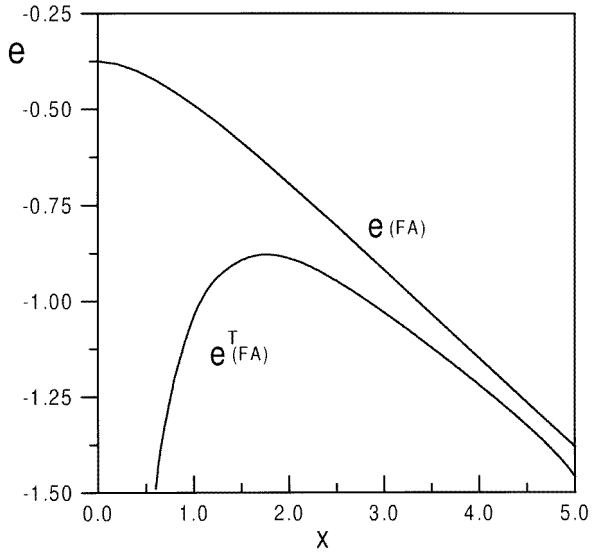

Figure 7. GS energy per site of the AF ladder and its T dual given by the FA ladder. Notice that inequality (68) is satisfied.

Finally, the S transformation is defined by the replacement of vertical bonds by horizontal ones and vice versa,

$$\begin{aligned} J_{\parallel}^{S} &= \tfrac{1}{2} J_{\perp} \langle \boldsymbol{S}_1(n) \cdot \boldsymbol{S}_2(n) \rangle / \langle \boldsymbol{S}_1(n) \cdot \boldsymbol{S}_1(n+1) \rangle \\ J_{\perp}^{S} &= 2 J_{\parallel} \langle \boldsymbol{S}_1(n) \cdot \boldsymbol{S}_1(n+1) \rangle / \langle \boldsymbol{S}_1(n) \cdot \boldsymbol{S}_2(n) \rangle. \end{aligned} \tag{69}$$

The factors 2 and $\frac{1}{2}$ are explained by the fact that there are two leg-bonds for each rung-bond.

In figure 8 we plot the energies of the AA ladder and its transformation which satisfy the inequality,

$$e_{\infty}(J_{\parallel}^{S}(AA), J_{\perp}^{S}(AA)) \leqslant e_{\infty}(J_{\parallel}(AA), J_{\perp}(AA)). \tag{70}$$

Note that in the region $J_{\parallel} \sim 0.7 J_{\perp}$ both energies get very close. In the crossing point of figure 8 the exchange energies associated to the rungs and the legs are the same. Figure 9 shows the spin correlation length for the AA ladder and its S transformed, displaying the same pattern as figure 8. We conclude that in the intermediate coupling regime the AA ladder is self-dual under S. This is a rather neat characterization of the GS of the usual antiferromagnetic ladder, whose GS is thought to be a realization of the RVB state. Indeed the GS of the 2×2 cluster with $J_{\perp} = J_{\parallel} > 0$ is indeed invariant under S which interchanges the rungs and the legs.

The discrete duality transformations allow us to understand the relations between ladders with different magnetic structures on a geometrical level. In the case of fermions living on a torus the modular group is a powerful tool to construct, for example, modular invariant partition functions. Spin ladders are rather different physical systems but one may wonder whether the discrete dualities could be exploited to further described properties of the ladders. This question requires further investigation which is beyond the purposes of this paper.

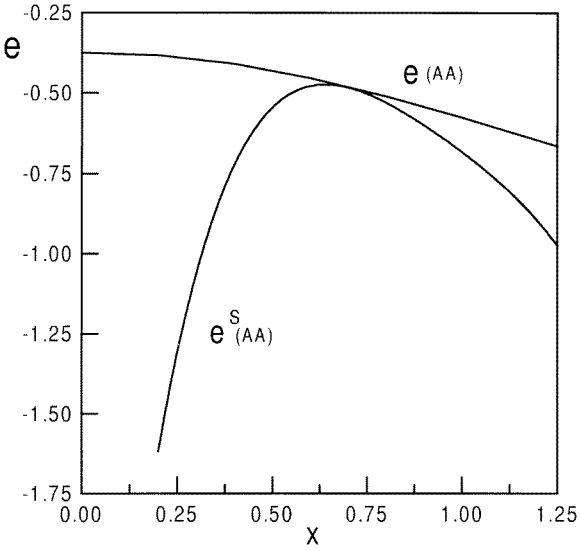

Figure 8. GS energy per site of the AA ladder and its S dual. Notice that the inequality (70) is satisfied.

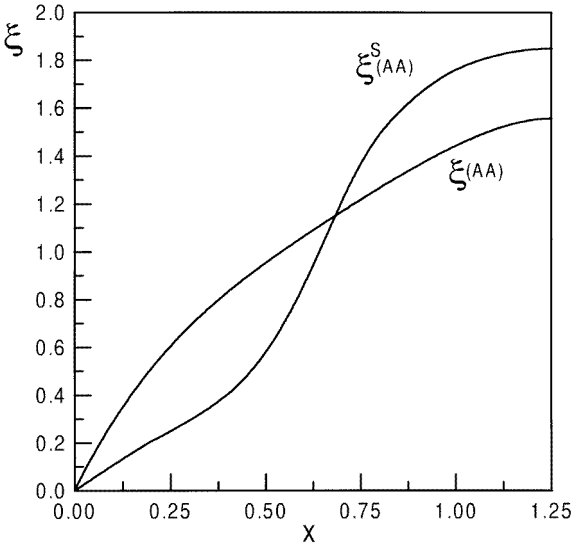

Figure 9. Spin correlation length of the AA ladder and its S dual.

4.5. AA_1 ladder: short-range string order

In table 5 we show the GS energy density and the spin correlation length of the ladder AA_1. Observe that the correlation length is longer that the one of the spin $\frac{1}{2}$ ladder.

As mentioned in the introduction a spin 1 chain has a long-range topological order (LRTO) characterized by a nonvanishing $g(\infty)$. In appendix C we give an analytical expression for $g(\infty)$ in terms of the MP parameters of the spin 1 chain.

However, when two spin 1 chains are coupled antiferromagnetically the LRTO

Table 5. GS energy per site and correlation length of the AA_1 ladder.

$J_\parallel/J_\perp$	$-e_\infty/2J_\perp$	ξ
0.0	1.000 000	0.000 00
0.2	1.055 719	1.011 4
0.4	1.206 557	1.831 8
0.6	1.407 358	2.385 2
0.8	1.631 166	2.676 2
1.0	1.867 327	2.822 7
1.25	2.172 905	2.904 2
1.66	2.688 880	2.928 6

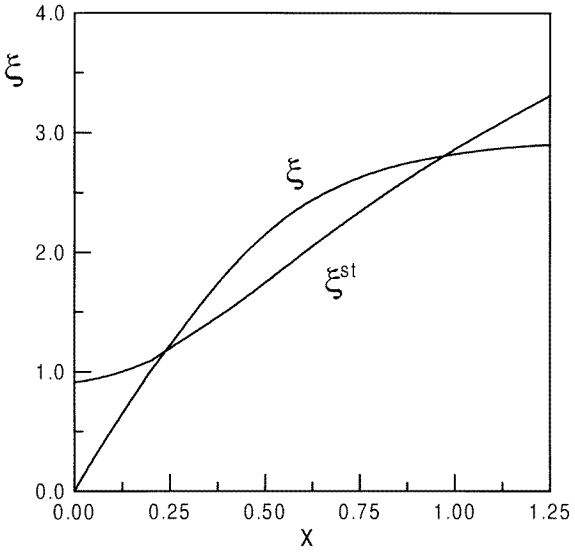

Figure 10. Plots of the spin correlation length ξ and the string correlation length $\xi^{\rm st}$ of the ladder AA_1. The latter quantity is computed using equations (125) and (126).

disappears and the string order parameter $g(\ell)$ decays exponentially as $e^{-\ell/\xi^{\rm st}}$. We call $\xi^{\rm st}$ the string correlation length, and its value together with the spin correlation length are shown in figure 10 as functions of the ratio $J_\parallel/J_\perp$. In the weak coupling limit where $J_\parallel/J_\perp \to \infty$ we expect $\xi^{\rm st}$ to diverge, recovering in that way the LRTO of the uncoupled chains. The value of $\xi^{\rm st}$ is obtained by the formula (19) with x_p the highest eigenvalue of the operator $e^{\widehat{i\pi S_1^z}}$ (see appendix C).

An intuitive way to understand the breaking of the LRTO is given by the AKLT picture of [3]. An AKLT state is a valence bond state where every spin 1 is represented as a symmetrized product of two spins $\frac{1}{2}$, such that everyone of these 'elementary' spins is linked by a bond to one of the spins $\frac{1}{2}$ on its neighbours. In this way all the spins of the chain are connected by a sucession of nearest-neighbour links. When we couple antiferromagnetically two spin 1 chains there is the possibility that two parallel bonds along the legs become two parallel bonds along the rungs, as shown in figure 11. Thus, the two infinite parallel arrays of connected bonds, characteristic of the uncoupled chains, effectively break into a collection of fluctuating islands whose size is of the order of $\xi^{\rm st}$. Everyone of these islands is a sort

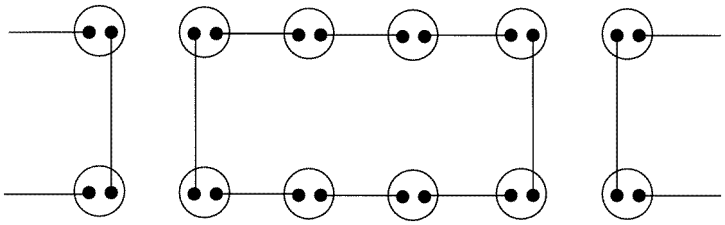

Figure 11. Pictorical representation of a possible AKLT state of the spin 1 ladder.

Table 6. GS energy per site and correlation length of the $AA_{3/2}$ ladder.

$J_\parallel/J_\perp$	$-e_\infty/2J_\perp$	ξ
0.0	1.875 000	0.0000
0.2	2.054 760	1.8760
0.4	2.449 827	3.3099
0.6	2.911 353	3.9475
0.8	3.400 562	4.2401
1.0	3.904 988	4.3829
1.25	4.548 607	4.4624
1.66	5.623 131	4.4900

of closed spin 1 chain (figure 11).

The finite value of ξ^{st} at the origin of figure 10 is due to the fact that $\mathrm{e}^{\mathrm{i}\pi S_1^z}$ has indeed a finite value when computed on the singlet formed by two spins 1 on a rung,

$$\langle \mathrm{e}^{\mathrm{i}\pi S_1^z}\rangle_{\mathrm{rung}} = \sum_{m=\pm 1,0} (-1)^m \langle 1m1-m|00\rangle^2 = -\tfrac{1}{3} \tag{71}$$

which leads to $\xi^{\mathrm{st}}(J_\parallel = 0) = 1/\ln 3$. Figure 10 suggests the existence of three different regimes. In the weak coupling regime where $\xi^{\mathrm{st}} > \xi$ the ladder can be effectively considered as a collection of weakly interacting closed spin 1 chains. In the strong coupling regime where $\xi^{\mathrm{st}} > \xi$ the bonds are mainly distributed along the rungs and the interbond coupling is small. Finally there is an intermediate region, with $\xi^{\mathrm{st}} < \xi$, where the islands of spins interact strongly with their neighbours.

4.6. The $AA_{3/2}$ ladder

In table 6 we give the GS energy densities and spin correlation lengths of the ladder $AA_{3/2}$. As one may expect the correlation length is longer than for the spin 1 and $\frac{1}{2}$ ladders. This fact agrees with the results obtained by mapping the spin ladders into the NLSM [16–18].

4.7. AKLT states for ladders

The spin $\frac{3}{2}$ two-legged ladder offers the possibility of constructing an AKLT state with a valence bond connecting every spin $\frac{3}{2}$ to its three nearest neighbours. More generally, let us consider a ladder with spin $S \geqslant \frac{3}{2}$ and three integers $p, q, r \geqslant 1$ satisfying the equation $2S = p + q + r$. Then one can define an AKLT state, denoted by the triplet (p, q, r), by linking the $2S$ 'elementary spinors' of each spin to the ones in its neighbours following the pattern shown in figure 12. The AKLT states (p, q, r) and (q, p, r) when $p \neq q$ correspond to dimerized ladders and they differ by the translation of one unit space along the legs.

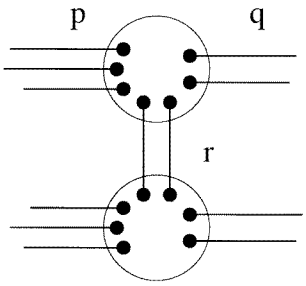

Figure 12. Graphical representation of a generic AKLT state of a ladder denoted as (p, q, r). There are a total of $p + q + r$ dots inside every circle representing a total spin $S = (p + q + r)/2$. The corresponding MP parameters are given by equation (75).

The spin $\frac{3}{2}$ AKLT ladder corresponds in the above notation to $(1, 1, 1)$. This state contains in fact a spin 0 and a spin 1 state which can be generated by the MP equation (35) where the amplitudes $A^{\lambda}_{J_1 J_2}$ are given by 9-j symbols,

$$A^{\lambda}_{J_1 J_2} = 3\sqrt{(2J_2+1)(2\lambda+1)} \begin{Bmatrix} 1/2 & 1/2 & J_2 \\ 3/2 & 3/2 & \lambda \\ 1 & 1 & J_1 \end{Bmatrix}. \tag{72}$$

In this equation J_1, $J_2 = 0$ and 1, while $\lambda = 0, 1, 2$.

The proof of (72) follows from the definition of the 9-j symbols as the coefficients that give the change of basis when coupling in two different ways four angular momenta, namely [31]

$$\psi(j_1 j_3 (J_{13}) j_2 j_4 (J_{24}) J) = \sum_{J_{12} J_{34}} \sqrt{(2J_{12}+1)(2J_{34}+1)(2J_{13}+1)(2J_{24}+1)} \times \begin{Bmatrix} j_1 & j_2 & J_{12} \\ j_3 & j_4 & J_{34} \\ J_{13} & J_{24} & J \end{Bmatrix} \psi(j_1 j_2 (J_{12}) j_3 j_4 (J_{34}) J) \tag{73}$$

where $\psi(j_1 j_3 (J_{13}) j_2 j_4 (J_{24}) J)$ is a state with angular momentum J obtained by the tensor product decomposition $J_{13} \otimes J_{24} \to J$, which in turn is obtained by the decompositions $j_1 \otimes j_3 \to J_{13}$ and $j_2 \otimes j_4 \to J_{24}$.

One may check that the normalization conditions (39) hold for (72), as a consequence of the orthogonality conditions satisfied by the 9-j symbols [31]. The GS energy per site and the spin correlation length of the AKLT state (72) in the case where $J_{\parallel} = J_{\perp} = J$ are given by,

$$e_{\infty}^{\mathrm{AKLT}}/2J = -3.263\,536 \qquad \xi^{\mathrm{AKLT}} = 1.116\,221. \tag{74}$$

This state has a much shorter correlation length than the MP state that minimizes the GS energy of the $AA_{3/2}$ ladder (see table 6). The GS energies of both states are also quite different. We conclude from these facts that the spin $\frac{3}{2}$ AKLT state does not give a good description of the GS of the $AA_{3/2}$ ladder.

A generic AKLT state of the type (p, q, r) when $p \neq q$ has to be described by alternating MP amplitudes depending on the evenness of the site. Thus for even sites one has

$$A^{\lambda}_{J_1 J_2} = (q + r + 1)\sqrt{(2J_2+1)(2\lambda+1)} \begin{Bmatrix} \frac{p}{2} & \frac{p}{2} & J_2 \\ S & S & \lambda \\ \frac{q+r}{2} & \frac{q+r}{2} & J_1 \end{Bmatrix} \tag{75}$$

where $J_1 = 0, \ldots, q$; $J_2 = 0, \ldots, p$ and $\lambda = 0, \ldots, 2S - r$. For odd sites the corresponding MP amplitudes are obtained by interchanging p and q in (75).

The fact that the MP amplitudes turn out to be given by 9-j symbols suggests a possible group theoretical interpretation of the AKLT states of the ladders. It would be interesting to

know what the values of the density matrix ρ_J as computed from equations (42) and (44) are. Another suggestion is that it might be possible to obtain AKLT states using the 9-j symbols of quantum groups in analogy to the construction of the IRF models in statistical mechanics in terms of the 6-j symbols of quantum groups (for a review on this subject see [32]).

5. Conclusions and prospects

Let us summarize the main results obtained in this paper.

• We have further developed the rotational invariant formulation of [5, 7]. By making use of all the powers of group theory we give explicit and managable formulae of the GS energy density, the correlation length and the string order parameter, in terms of invariant objects like 6-j symbols, etc. This reduces considerably the number of independent MP parameters used in the minimization process. Our work gives the MP version of the IRF-DMRG method developed in [33], where it was shown how to apply the DMRG to Hamiltonians invariant under a Lie group or a quantum group as for example the Heisenberg model or the quantum group invariant XXZ chain.

• We have improved the numerical results concerning the GS energy density and spin correlation length obtained previously with other approximate methods as those of [24, 23]. In particular, we have proved that the ansätzse generated by first-order recursion relations, like the MPM, are better than those generated by second- or higher-order recursion relations as those of [24]. Moreover, MP ansätzse with multiple states per spin greatly improved the numerical results. In this sense the multiplicity of states kept in the construction seems to be a key ingredient in the DMRG.

• We have shown the equivalence between the ladder $AF_{1/2}$ and the spin 1 antiferromagnetic Heisenberg chain. The MPM applied to both systems shows strong numerical coincidences for the GS energy and correlation length. This agrees with the results obtained previously by other methods [26–28].

• We have found numerical evidences for the duality properties proposed in [29] for the spin ladders with magnetic structures AA, AF and FA.

• We have shown that there is a breaking of the long range topological order of the spin 1 chains when they are coupled in a two-legged ladder. A physical picture of the GS of the spin 1 ladder is given in terms of resonating closed spin 1 chains.

• We have constructed AKLT states for two-legged ladders with spin $S \geqslant \frac{3}{2}$, showing that the corresponding MP parameters are given by 9-j symbols. This gives a group theoretical meaning to the MP variational parameters.

• Besides using the MPM as a computational tool to solve physical problems we have tried to make further progress in the formal understanding of why the DMRG works so well. Elaborating the ideas first presented in [7] we suggest that one can possibly give a derivation of the infinity system algorithm by starting from the MPM. As we have shown in section 2, both in the DMRG and the MPM, there appears a density matrix playing a central role.

In summary we have shown the adequacy of the MPM to study the two-legged ladder, especially in the strong and intermediate coupling regimes. This is made possible by the fact that these ladders are finitely correlated. Hence, one may expect that even spin ladders with a finite number of legs could be described by the same technique, although with a larger number of states m. On the other hand, odd-legged ladders are not finitely correlated and they cannot be properly described in the large N limit within the actual formulation of the MPM. An interesting problem is the application of the MPM to 2D systems, which can be thought of as ladders with a large number of legs. It is clear that one should choose a

collection of the most representative states for the rungs to be added after each iteration of the MP recurrence equation.

Acknowledgments

JMR acknowledges financial support from a Basque Government FPI grant as well as from CICYT, contract AEN95-0590, and CIRIT, contract GRQ93-1047. He also thanks G Sierra, J Dukelsky and M A Martín-Delgado for hospitality at the IMAFF (CSIC), Madrid, where this work was performed. GS and MAMD acknowledges support from the DIGICYT under contract no PB96/0906 and JD acknowledges support from the DIGICYT under contract no PB95/0123.

Appendix A: The MP ansatz and the Grassmannian manifolds

In this appendix we shall give a proof of equation (4) which gives a precise mathematical meaning of the coefficients $A_{\alpha\beta}[s]$ defining a generic MP ansatz.

In the r.h.s. of equation (1) we have a generic vector of dimension $n = mm^*$ while on its l.h.s. the vector has dimension m. Hence equation (1) amounts to a choice of a m-dimensional linear subspace of $\mathbb{R}^n$ in the case of $A_{\alpha\beta}[s]$ real or a complex subspace of $\mathbb{C}^n$ in the case of $A_{\alpha\beta}[s]$ complex. Let us call the set of all these subspaces as $M_{n,m}(\mathbb{R})$ and $M_{n,m}(\mathbb{C})$ for $A_{\alpha\beta}[s]$ real and complex, respectively. The group $O(n)$ (resp. $U(n)$) acts transitively on $M_{n,m}(\mathbb{R})$ (resp. $M_{n,m}(\mathbb{C})$), which leads to the result [34]

$$M_{n,m}(\mathbb{R}) = \frac{O(n)}{O(m) \otimes O(n-m)} \tag{76}$$

$$M_{n,m}(\mathbb{C}) = \frac{U(n)}{U(m) \otimes U(n-m)}. \tag{77}$$

In (76) the groups $O(m)$ and $O(n-m)$ are identified with the subgroups of $O(n)$ consisting of those elements leaving fixed every vector of a given $(n-m)$-dimensional subspace and of its orthogonal complement, respectively. Similar arguments lead to equation (77). $M_{n,m}(\mathbb{R})(M_{n,m}(\mathbb{C}))$ are called the real (complex) Grassmannian manifolds. Taking $n = mm^*$ in (76) we get equation (4).

As a simple illustration of these eqs. let us consider the case of a MP ansatz that generates a single state $|GS\rangle_N$ $(m = 1)$, i.e.

$$|GS\rangle_N = \sum_s A[s]|s\rangle_N \otimes |GS\rangle_{N-1} \tag{78}$$

with $A[s] \in \mathbb{R}$. The normalization condition (2) reads,

$$\sum_{s=1}^{m^*} A[s]^2 = 1. \tag{79}$$

Thus $A[s]$ belongs to the (m^*-1)-dimensional sphere $SO(m^*)/SO(m^*-1)$. Upon the identification of $A[s]$ and $-A[s]$ we get the (m^*-1)-real proyective space $M_{m^*,1}(\mathbb{R}) = SO(m^*)/SO(m^*-1) \otimes \mathbb{Z}_2$.

Appendix B: The rotational invariant MPM

Group theoretical preliminaries

Before we give the proof of the main formulae of section 3 we shall review some basic definitions and results in group theory [31].

An irreducible tensor with angular momentum k is an operator $T^{(k)}_M (M = k, \ldots, -k)$ which satisfies the following commutation relations with the total angular momentum operator $\boldsymbol{J}$,

$$\begin{aligned} &[J_z, T^{(k)}_M] = M T^{(k)}_M \\ &[J_x \pm i J_y, T^{(k)}_M] = \sqrt{k(k+1) - M(M \pm 1)}\, T^{(k)}_{M\pm 1}. \end{aligned} \tag{80}$$

The scalar product of two irreducible tensors $\boldsymbol{T}^{(k)}$ and $\boldsymbol{U}^{(k)}$ with the same spin k is defined by,

$$\boldsymbol{T}^{(k)} \cdot \boldsymbol{U}^{(k)} = \sum_{M=-k}^{k} (-1)^{-M} T^{(k)}_M U^{(k)}_{-M}. \tag{81}$$

The Wigner–Eckart theorem reads,

$$\langle JM | T^{(k)}_\mu | J'M' \rangle = (-1)^{J-M} \begin{pmatrix} J & k & J' \\ -M & \mu & M' \end{pmatrix} (J || \boldsymbol{T}^{(k)} || J') \tag{82}$$

where the 3-j symbol is related to the CG coefficient by

$$\begin{pmatrix} J & k & J' \\ -M & \mu & M' \end{pmatrix} = \frac{(-1)^{J-k-M'}}{\sqrt{2J'+1}} \langle J - M k \mu | J' - M' \rangle. \tag{83}$$

The quantity $(J||\boldsymbol{T}^{(k)}||J')$ in (82) is called the reduced matrix element of the operator $\boldsymbol{T}^{(k)}$. As an example we give the reduced matrix element of the spin operator $\boldsymbol{S}$,

$$(S||\boldsymbol{S}||S) = \sqrt{S(S+1)(2S+1)}. \tag{84}$$

Let $|\alpha_1 j_1 \alpha_2 j_2 J M\rangle$ be a state with total angular momenta J and third component M, appearing in the tensor product decomposition $(\alpha_1 j_1) \otimes (\alpha_2 j_2)$, where (αj) denotes a state with total angular momentum j and α labels other possible quantum numbers. We shall require the following results:

$$\begin{aligned} \langle \alpha_1 j_1 \alpha_2 j_2 J M | (\boldsymbol{T}^{(k)}_1 \cdot \boldsymbol{T}^{(k)}_2) | \alpha_1' j_1' \alpha_2' j_2' J' M' \rangle &= \delta_{JJ'} \delta_{MM'} (-1)^{j_2 + J + j_1'} \begin{Bmatrix} j_1 & j_2 & J \\ j_2' & j_1' & k \end{Bmatrix} \\ &\times (\alpha_1 j_1 || \boldsymbol{T}^{(k)}_1 || \alpha_1' j_1') (\alpha_2 j_2 || \boldsymbol{T}^{(k)}_2 || \alpha_2' j_2') \end{aligned} \tag{85}$$

$$\begin{aligned} (\alpha_1 j_1 \alpha_2 j_2 J || \boldsymbol{T}^{(k)}_1 || \alpha_1' j_1' \alpha_2' j_2' J') &= \delta_{\alpha_2 \alpha_2'} \delta_{j_2 j_2'} (-1)^{j_1 + j_2 + J' + k} \begin{Bmatrix} j_1 & J & j_2 \\ J' & j_1' & k \end{Bmatrix} \\ &\times \sqrt{(2J+1)(2J'+1)} (\alpha_1 j_1 || \boldsymbol{T}^{(k)}_1 || \alpha_1' j_1') \end{aligned} \tag{86}$$

$$\begin{aligned} (\alpha_1 j_1 \alpha_2 j_2 J || \boldsymbol{T}^{(k)}_2 || \alpha_1' j_1' \alpha_2' j_2' J') &= \delta_{\alpha_1 \alpha_1'} \delta_{j_1 j_1'} (-1)^{j_1 + j_2' + J + k} \begin{Bmatrix} j_2 & J & j_1 \\ J' & j_2' & k \end{Bmatrix} \\ &\times \sqrt{(2J+1)(2J'+1)} (\alpha_2 j_2 || \boldsymbol{T}^{(k)}_2 || \alpha_2' j_2'). \end{aligned} \tag{87}$$

The subindices 1 and 2 in $\boldsymbol{T}^{(k)}_1$ and $\boldsymbol{T}^{(k)}_2$ mean that the corresponding operators acts on the states labelled as $(\alpha_1 j_1)$ and $(\alpha_2 j_2)$ respectively.

Proof. We want to prove equation (41).

Using equation (35) we easily get for $N > n > m$,

$$ {}_N\langle J_1M|\mathcal{O}^{(k,A)}(n)\cdot\mathcal{O}^{(k,B)}(m)|J_1M\rangle_N = \sum_{J_2} T_{J_1,J_2N-1}\langle J_2M|\mathcal{O}^{(k,A)}(n)\cdot\mathcal{O}^{(k,B)}(m)|J_2M\rangle_{N-1} \tag{88} $$

where T_{J_1,J_2} is given in (42). Iterating (88) $N-n$ times we reach the situation where $N=n$. This produces the term $T^{N-n}_{J_1,J_2}$ in (41). Next we need to compute the matrix element,

$$ \begin{aligned} {}_n\langle J_1M|\mathcal{O}^{(k,A)}(n)\cdot\mathcal{O}^{(k,B)}(m)|J_1M\rangle_n &= \sum_{J_2J_3\lambda_2\lambda_3} (A^{\lambda_2}_{J_1J_2})^* A^{\lambda_3}_{J_1J_3} \\ &\times {}_n\langle(\lambda_2J_2),\, J_1M|\mathcal{O}^{(k,A)}(n)\cdot\mathcal{O}^{(k,B)}(m)|(\lambda_3J_3),\, J_1M\rangle_n. \end{aligned} \tag{89} $$

The matrix element on the r.h.s. of (89) has the form described in (85), which yields,

$$ \begin{aligned} {}_n\langle(\lambda_2J_2),\, J_1M|\mathcal{O}^{(k,A)}(n)\cdot\mathcal{O}^{(k,B)}(m)|(\lambda_3J_3),\, J_1M\rangle_n &= (-1)^{J_1+J_2+\lambda_3}\begin{Bmatrix}\lambda_2 & J_2 & J_1\\ J_3 & \lambda_3 & k\end{Bmatrix} \\ &\times {}_n(\lambda_2||\mathcal{O}^{(k,A)}(n)||\lambda_3)_{nn-1}(J_2||\mathcal{O}^{(k,B)}(m)||J_3)_{n-1}. \end{aligned} \tag{90} $$

Introducing (90) into (89) we find

$$ {}_n\langle J_1M|\mathcal{O}^{(k,A)}(n)\cdot\mathcal{O}^{(k,B)}(m)|J_1M\rangle_n = \sum_{J_2J_3}\hat{\mathcal{O}}^{(k,A)}_{J_1,J_2J_3n-1}(J_2||\mathcal{O}^{(k,B)}(m)||J_3)_{n-1} \tag{91} $$

where

$$ \hat{\mathcal{O}}^{(k,A)}_{J_1,J_2J_3} = \sum_{\lambda_2,\lambda_3}(A^{\lambda_2}_{J_1J_2})^* A^{\lambda_3}_{J_1J_3}\times(-1)^{\lambda_3+J_1+J_2}\begin{Bmatrix}\lambda_2 & J_2 & J_1\\ J_3 & \lambda_3 & k\end{Bmatrix}(\lambda_2||\mathcal{O}^{(k,A)}||\lambda_3). \tag{92} $$

The next step is to apply the MP ansatz (35) to

$$ {}_n(J_1||\mathcal{O}^{(k,B)}(m)||J_2)_n = \sum_{\lambda_1\lambda_2}(A^{\lambda_1}_{J_1J_3})^* A^{\lambda_2}_{J_2J_4}\times_n((\lambda_1J_3),\, J_1||\mathcal{O}^{(k,B)}(m)||(\lambda_2J_4),\, J_2)_n. \tag{93} $$

For $n > m$ we can use (87), obtaining

$$ \begin{aligned} {}_n((\lambda_1J_3),\, J_1||\mathcal{O}^{(k,B)}(m)||(\lambda_2J_4),\, J_2)_n &= \delta_{\lambda_1\lambda_2}(-1)^{\lambda_1+J_1+J_4+k}\sqrt{(2J_1+1)(2J_2+1)} \\ &\times\begin{Bmatrix}J_3 & J_1 & \lambda_1\\ J_2 & J_4 & k\end{Bmatrix}_{n-1}(J_3||\mathcal{O}^{(k,B)}(m)||J_4)_{n-1}. \end{aligned} \tag{94} $$

Plugging (94) into (93) we get,

$$ {}_n(J_1||\mathcal{O}^{(k,B)}(m)||J_2)_n = \sum_{J_3J_4}(T_k)_{J_1J_2,J_3J_4n-1}(J_3||\mathcal{O}^{(k,B)}(m)||J_4)_{n-1},\ (n>m) \tag{95} $$

where $(T_k)_{J_1J_2,J_3J_4}$ is defined in (43). The term T_k^{n-m-1} in (41) results from the iteration of (95) until one gets $n=m$. In the case when $n=m$ in (94) we should apply (86) obtaining

$$ \begin{aligned} {}_n((\lambda_1J_3),\, J_1||\mathcal{O}^{(k,B)}(n)||(\lambda_2J_4),\, J_2)_n &= \delta_{J_3J_4}(-1)^{\lambda_1+J_2+J_3+k}\sqrt{(2J_1+1)(2J_2+1)} \\ &\times\begin{Bmatrix}\lambda_1 & J_1 & J_3\\ J_2 & \lambda_2 & k\end{Bmatrix}_n(\lambda_1||\mathcal{O}^{(k,B)}(n)||\lambda_2)_n. \end{aligned} \tag{96} $$

Introducing (96) into (93) we get,

$$ {}_n(J_1||\mathcal{O}^{(k,B)}(n)||J_2)_n = \sum_{J_3}\hat{\mathcal{O}}^{(k,B)}_{J_1J_2,J_3} \tag{97} $$

where

$$\hat{\mathcal{O}}^{(k,B)}_{J_1J_2,J_3} = \sum_{\lambda_1\lambda_2} (A^{\lambda_1}_{J_1J_3})^* A^{\lambda_2}_{J_2J_3} (-1)^{\lambda_1+J_2+J_3+k} \times \sqrt{(2J_1+1)(2J_2+1)} \begin{Bmatrix} \lambda_1 & J_1 & J_3 \\ J_2 & \lambda_2 & k \end{Bmatrix} (\lambda_1 || \mathcal{O}^{(k,B)} || \lambda_2). \tag{98}$$

This ends the proof of equation (41). □

Recursion relation of the energy expectation values

We shall not give here the explicit proof of equation (50) since it is quite analogous to the one performed in the previous paragraph. We shall simply state the result.

The matrix $\hat{h}_{J_1,J_2}$ appearing in (50) is given by the sum

$$\hat{h}_{J_1,J_2} = \hat{h}^{(1)}_{J_1,J_2} + \hat{h}^{(2)}_{J_1,J_2} \tag{99}$$

where

$$\hat{h}^{(1)}_{J_1,J_2} = J_\perp \sum_\lambda (\tfrac{1}{2}\lambda(\lambda+1) - S(S+1)) |A^\lambda_{J_1J_2}|^2 \tag{100}$$

$$\hat{h}^{(2)}_{J_1,J_4} = 2J_\parallel \sum_{J_2J_3J_4,\lambda_1,\ldots,\lambda_4} (A^{\lambda_1}_{J_1J_2} A^{\lambda_3}_{J_2J_4})^* A^{\lambda_2}_{J_1J_3} A^{\lambda_4}_{J_3J_4} \times (-1)^{1+\lambda_3+\lambda_4} \xi^{\lambda_2\lambda_1}_{J_2J_3J_1} \xi^{\lambda_3\lambda_4}_{J_3J_2J_4} \tag{101}$$

and

$$\xi^{\lambda_1\lambda_2}_{J_1J_2J_3} = (-1)^{J_1+J_3} \sqrt{(2J_1+1)(2\lambda_1+1)(2\lambda_2+1)} \times \sqrt{S(S+1)(2S+1)} \begin{Bmatrix} \lambda_1 & \lambda_2 & 1 \\ J_1 & J_2 & J_3 \end{Bmatrix} \begin{Bmatrix} \lambda_1 & \lambda_2 & 1 \\ S & S & S \end{Bmatrix}$$

where the following property for the 6-j symbol with an element equal to 1 has been used [31]:

$$\begin{Bmatrix} \lambda_1 & \lambda_2 & 1 \\ J_1 & J_2 & J_3 \end{Bmatrix} = \begin{Bmatrix} \lambda_2 & \lambda_1 & 1 \\ J_2 & J_1 & J_3 \end{Bmatrix}.$$

Appendix C: the string order parameter of spin 1 chain and ladder

Let us first consider the spin 1 chain. The MP ansatz is given simply by,

$$|J_1M_1\rangle_N = \sum_{J_2} A_{J_1J_2} |(1J_2),\, J_1M_1\rangle_N \tag{102}$$

where the state $|(1J_2),\, J_1M_1\rangle_N$ reads as in (36) with $\lambda = 1$. We shall choose half-integer values of the angular momenta J_1 and J_2 which amounts to have a spin $\frac{1}{2}$ at one end of the chain [5, 7].

We shall next show that the operators $T = \hat{1}$ and $\widehat{e^{i\pi S^z}}$ both have an eigenvalue equal to 1. Let us first of all explicitly write their components,

$$(T)_{J_1M_1J_1'M_1',J_2M_2J_2'M_2'} = \delta_{M_1-M_2,M_1'-M_2'} A_{J_1J_2} A_{J_1'J_2'} \times \langle 1M_1 - M_2,\, J_2M_2 | J_1M_1\rangle \langle 1M_1' - M_2',\, J_2'M_2' | J_1'M_1'\rangle \tag{103}$$

$$(\widehat{e^{i\pi S^z}})_{J_1M_1J_1'M_1',J_2M_2J_2'M_2'} = \delta_{M_1-M_2,M_1'-M_2'} (-1)^{M_1-M_2} A_{J_1J_2} A_{J_1'J_2'} \times \langle 1M_1 - M_2,\, J_2M_2 | J_1M_1\rangle \langle 1M_1' - M_2',\, J_2'M_2' | J_1'M_1'\rangle. \tag{104}$$

The normalization conditions on $A_{J_1J_2}$ read

$$\sum_{J_2} A^2_{J_1J_2} = 1 \qquad \forall J_1. \tag{105}$$

Using these equations and the properties of the CG coefficients, one can verify that v and $v^{\rm st}$ defined as

$$\begin{aligned} v_{J_1M_1J_1'M_1'} &= \delta_{J_1J_1'}\delta_{M_1M_1'} \\ v^{\rm st}_{J_1M_1J_1'M_1'} &= \delta_{J_1J_1'}\delta_{M_1M_1'}(-1)^{M_1-1/2} \end{aligned} \tag{106}$$

are right eigenvectors with eigenvalue 1 of the matrices T and $\widehat{e^{i\pi S^z}}$ respectively.

Similarly, the left eigenvectors associated to this eigenvalue are given by,

$$\begin{aligned} \rho_{J_1M_1J_1'M_1'} &= \delta_{J_1J_1'}\delta_{M_1M_1'}\rho_{J_1}/(2J_1+1) \\ \rho^{\rm st}_{J_1M_1J_1'M_1'} &= \delta_{J_1J_1'}\delta_{M_1M_1'}(-1)^{M_1-1/2}\rho_{J_1}/(2J_1+1) \end{aligned} \tag{107}$$

where ρ_J is the left eigenvector with eigenvalue 1 of the matrix $T_{J_1J_2} = A^2_{J_1J_2}$.

According to equation (22) the string order parameter $g(\infty)$ is given by the product of two matrix elements which we compute below.

Let us first consider,

$$\langle\rho|\widehat{S^z}|v^{\rm st}\rangle = \sum \rho_{J_1M_1J_1'M_1'}\widehat{S^z}_{J_1M_1J_1'M_1',J_2M_2J_2'M_2'}v^{\rm st}_{J_2M_2J_2'M_2'}. \tag{108}$$

The hated version of S^z is given by,

$$\begin{aligned} (\widehat{S^z})_{J_1M_1J_1'M_1',J_2M_2J_2'M_2'} &= \delta_{M_1-M_2,M_1'-M_2'}(M_1-M_2)A_{J_1J_2}A_{J_1'J_2'} \\ &\quad\times\langle 1M_1-M_2,\, J_2M_2|J_1M_1\rangle\langle 1M_1'-M_2',\, J_2'M_2'|J_1'M_1'\rangle \end{aligned} \tag{109}$$

which together with (107), (108) lead to,

$$\langle\rho|\widehat{S^z}|v^{\rm st}\rangle = \sum \frac{\rho_{J_1}}{2J_1+1}A^2_{J_1J_2}\times(-1)^{M_2-1/2}(M_1-M_2)(\langle 1M_1-M_2,\, J_2M_2|J_1M_1\rangle)^2. \tag{110}$$

Similarly we get

$$\langle\rho^{\rm st}|\widehat{S^z}|v\rangle = \sum \frac{\rho_{J_1}}{2J_1+1}A^2_{J_1J_2}\times(-1)^{M_1-1/2}(M_1-M_2)(\langle 1M_1-M_2,\, J_2M_2|J_1M_1\rangle)^2. \tag{111}$$

Observing that

$$(-1)^{M_1-1/2}(M_1-M_2) = -(-1)^{M_2-1/2}(M_1-M_2) \tag{112}$$

where $M_1-M_2 = 0, \pm 1$, we obtain

$$\langle\rho^{\rm st}|\widehat{S^z}|v\rangle = -\langle\rho|\widehat{S^z}|v^{\rm st}\rangle \tag{113}$$

which in turn implies

$$g(\infty) = -(\langle\rho|\widehat{S^z}|v^{\rm st}\rangle)^2. \tag{114}$$

Let us return to equation (110), which can be written as

$$\sum \frac{-\rho_{J_1}}{2J_1+1}A^2_{J_1J_2}(-1)^{M_1-1/2}\langle(1J_2)J_1M_1|S_1^z|(1J_2)J_1M_1\rangle \tag{115}$$

where S_1^z denotes the spin operator acting on the spin 1. Using the Wigner–Eckart theorem we get,

$$\begin{aligned} \langle(1J_2)J_1M_1|S_1^z|(1J_2)J_1M_1\rangle &= (-1)^{J_1-M_1}\begin{pmatrix} J_1 & 1 & J_1 \\ -M_1 & 0 & M_1 \end{pmatrix}((1J_2)J_1||\boldsymbol{S}_1||(1J_2)J_1) \\ &= \frac{M_1}{\sqrt{J_1(2J_1+1)(J_1+1)}}((1J_2)J_1||\boldsymbol{S}_1||(1J_2)J_1). \end{aligned} \tag{116}$$

The reduced matrix element appearing in (116) can be computed using (86),

$$((1J_2)J_1||\boldsymbol{S}_1||(1J_2)J_1) = \sqrt{6}(-1)^{J_1+J_2}(2J_1+1)\begin{Bmatrix} 1 & J_1 & J_2 \\ J_1 & 1 & 1 \end{Bmatrix}$$
$$= \frac{\sqrt{2J_1+1}(2+J_1(J_1+1)-J_2(J_2+1))}{2\sqrt{J_1(J_1+1)}}. \tag{117}$$

Substituting (116), (117) into (115) and performing the sum over M_1 with the aid of the formula,

$$\sum_{M=-J}^{J} M(-1)^{M-\frac{1}{2}} = (J+\tfrac{1}{2})(-1)^{J-1/2} \qquad (J:\text{ half integer}) \tag{118}$$

we finally get

$$\langle\rho|\widehat{S^z}|v^{\mathrm{st}}\rangle = \tfrac{1}{4}\sum \rho_{J_1} A^2_{J_1J_2}(-1)^{J_1-1/2} \times \frac{2+J_1(J_1+1)-J_2(J_2+1)}{J_1(J_1+1)}. \tag{119}$$

From equations (114), (119) we immediately get the value of $g(\infty)$ in the AKLT case,

$$\text{AKLT}: A_{\frac{1}{2}\frac{1}{2}} = 1 \rightarrow g(\infty) = -(\tfrac{2}{3})^2. \tag{120}$$

In [7] the spin 1 Heisenberg chain was studied with a MP ansatz built up with two states with $J = \frac{1}{2}$ and $\frac{3}{2}$. The values of the MP parameters obtained in [7] are reproduced below

$$\begin{aligned} &A_{\frac{1}{2}\frac{1}{2}} = 0.988\,995 \qquad A_{\frac{1}{2}\frac{3}{2}} = 0.147\,95 \\ &A_{\frac{3}{2}\frac{1}{2}} = -0.952\,887 \qquad A_{\frac{3}{2}\frac{3}{2}} = -0.303\,325 \\ &\rho_{\frac{1}{2}} = 0.976\,46 \qquad \rho_{\frac{3}{2}} = 0.023\,539. \end{aligned} \tag{121}$$

Introducing (121) into equations (114) and (119) we get $g(\infty) = -0.387$, which can be compared with the exact value given by $-0.374\,325$ [11]. In [5] the spin 1 chain was studied with a MP ansatz with two spin $\frac{1}{2}$ and two spin $\frac{3}{2}$ states, which yields $g(\infty) = -0.3759$. This shows again that MP ansätzse with multiplicity improve considerably the accuracy of the numerical results [5, 7].

Let us go now to the spin 1 ladder. In section 4 we gave an intuitive argument which suggested that the LRTO of the single spin 1 chains is destroyed by the interchain coupling. Next we show that this is indeed what happens.

Let us first write equations (103), (104) in the case of ladders

$$(T)_{J_1M_1J_1'M_1',J_2M_2J_2'M_2'} = \delta_{M_1-M_2,M_1'-M_2'}\sum_{\lambda} A^{\lambda}_{J_1J_2}A^{\lambda}_{J_1'J_2'}$$
$$\times\langle\lambda M_1-M_2,\, J_2M_2|J_1M_1\rangle\langle\lambda M_1'-M_2',\, J_2'M_2'|J_1'M_1'\rangle \tag{122}$$

$$(\widehat{\mathrm{e}^{\mathrm{i}\pi S_1^z}})_{J_1M_1J_1'M_1',J_2M_2J_2'M_2'} = \delta_{M_1-M_2,M_1'-M_2'}\sum_{\lambda\lambda'} A^{\lambda}_{J_1J_2}A^{\lambda'}_{J_1'J_2'}$$
$$\times\langle 1M_1-M_2,\, J_2M_2|J_1M_1\rangle\langle 1M_1'-M_2',\, J_2'M_2'|J_1'M_1'\rangle$$
$$\times\langle\lambda M_1-M_2|\mathrm{e}^{\mathrm{i}\pi S_1^z}|\lambda' M_1M_2\rangle \tag{123}$$

where S_1^z denotes the spin operator acting on the first leg of the ladder. The vector $v_{J_1M_1J_1'M_1'}$ given in (106) is an eigenvector with eigenvalue 1 of the matrix T defined by (122). This property is a consequence of the normalization condition (39). For the spin 1 chain the latter condition also guarantees the existence of an eigenvalue 1 of the operator (104). However, this is not generally the case for the operator (123).

The last matrix element in (123) can be deduced by expressing the state $|\lambda\mu\rangle$ of the rung in terms of the spin 1 states of every site,

$$|\lambda\mu\rangle = \sum_{m_1 m_2} |1m_1\rangle_1 |sm_2\rangle_2 \langle 1m_1 1m_2|\lambda\mu\rangle. \tag{124}$$

We thus get

$$\begin{aligned}(\widehat{\mathrm{e}^{\mathrm{i}\pi S_1^z}})_{J_1 M_1 J_1' M_1', J_2 M_2 J_2' M_2'} = \delta_{M_1 - M_2, M_1' - M_2'} \sum_{\lambda\lambda' m_1 m_2} A^{\lambda}_{J_1 J_2} A^{\lambda'}_{J_1' J_2'} (-1)^{m_1} \\ \times \langle 1M_1 - M_2,\, J_2 M_2 | J_1 M_1\rangle \langle 1M_1' - M_2',\, J_2' M_2' | J_1' M_1'\rangle \\ \times \langle 1m_1 1m_2 | \lambda M_1 - M_2\rangle \langle 1m_1 1m_2 | \lambda' M_1 - M_2\rangle\rangle. \end{aligned} \tag{125}$$

We can actually set up $M_1 = M_1'$ and $M_2 = M_2'$ in (125) since in the computation of the string order parameter, the third component of the angular momenta is preserved. We have computed the highest eigenvalue x_{st} of the matrix (125), which turns out to be smaller than 1. This shows that $g(\ell)$ decays exponentially with a correlation length ξ^{st} whose value is obtained by the equation

$$\xi^{\mathrm{st}} = -1/\ln|x_{\mathrm{st}}|. \tag{126}$$

References

[1] Wilson K G 1975 *Rev. Mod. Phys.* **47** 773
[2] White S R 1992 *Phys. Rev. Lett.* **69** 2863
White S R 1993 *Phys. Rev.* B **48** 10345
[3] Affleck I, Kennedy T, Lieb E H and Tasaki H 1988 *Commun. Math. Phys.* **115** 477
[4] Klümper A, Schadschneider A and Zittartz J 1993 *Europhys. Lett.* **24** 293
[5] Ostlund S and Rommer S 1995 *Phys. Rev. Lett.* **75** 3537
Rommer S and Ostlund S 1997 *Phys. Rev.* B **55** 2164
[6] Fannes M, Nachtergaele B and Werner R F 1992 *Commun. Math. Phys.* **144** 443 (see references therein on the MPM)
[7] Dukelsky J, Martín-Delgado M A, Nishino T and Sierra G 1998 *Europhys. Lett.* **43** 457
[8] Brehmer S, Mikeska H-J and Neugebauer U 1996 *J. Phys.: Condens. Matter* **8** 7161
[9] Dagotto E and Rice T M 1996 *Science* **271** 618
[10] den Nijs M and Rommelse K 1989 *Phys. Rev.* B **40** 4709
[11] White S R and Huse D A 1993 *Phys. Rev.* B **48** 3844
[12] Nishino T and Okunishi K 1996 *J. Phys. Soc. Japan* **65** 891
[13] Schulz H J 1986 *Phys. Rev.* B **34** 6372
[14] Strong S P and Millis A J 1992 *Phys. Rev. Lett.* **69** 2419
[15] Shelton D G, Nersesyan A A and Tsvelik A M 1996 *Phys. Rev.* B **53** 8521
[16] Senechal D 1995 *Phys. Rev.* B **52** 15 319
[17] Sierra G 1996 *J. Phys. A: Math. Gen.* **29** 3299
[18] Dell'Aringa S, Ercolessi E, Morandi G, Pieri P and Roncaglia M 1997 *Phys. Rev. Lett.* **78** 2457
[19] Dagotto E, Riera J and Scalapino D J 1992 *Phys. Rev.* B **45** 5744
[20] White S R, Noack R M and Scalapino D J 1994 *Phys. Rev. Lett.* **73** 886
[21] Frischmuth B, Ammon B and Troyer M 1996 *Phys. Rev.* B **54** R3714
[22] Greven M, Birgeneau R J and Wiese U-J 1996 *Phys. Rev. Lett.* **77** 1865
[23] Gopalan S, Rice T M and Sigrist M 1994 *Phys. Rev.* B **49** 8901
Normand B and Rice T M 1997 *Preprint* cond-mat/9701202
[24] Sierra G and Martín-Delgado M A 1997 *Phys. Rev.* B **56** 8774
[25] Barnes T, Dagotto E, Riera J and Swanson E S 1993 *Phys. Rev.* B **47** 3196
[26] Hida K 1991 *J. Phys. Soc. Japan* **60** 1347
[27] White S R 1996 *Phys. Rev.* B **53** 52
[28] Watanabe H 1995 *Phys. Rev.* B **52** 12 508
[29] Sierra G and Martín-Delgado M A 1998 *J. Phys. A: Math. Gen.* **31** 1657

[30] Ginsparg P 1990 *Les Houches Lecture Notes on Fields and Critical Phenomena* ed E Brezin and J Zinn-Justin (Amsterdam: North-Holland)
[31] Varshalovich D A, Moskalev A N and Khersonskii V K 1988 *Quantum Theory of Angular Momenta* (Singapore: World Scientific)
[32] Gomez C, Ruiz-Altaba M and Sierra G 1996 *Quantum Groups in Two-Dimensional Physics* (Cambridge: Cambridge University Press)
[33] Sierra G and Nishino T 1997 *Nucl. Phys.* B **495** [FS] 505
[34] Iyanaga S and Kawada Y (ed) 1977 *Encyclopedic Dictionary of Mathematics* (London: MIT)